PNNL-26924, Rev. 1

NDE Technology Development Program for Non-Visual Volumetric Inspection Technology

Phase I Summary Report

January 2018

KM Denslow
TL Moran
MR Larche
SW Glass

Prepared for the U.S. Department of Energy
under Contract DE-AC05-76RL01830

PACIFIC NORTHWEST NATIONAL LABORATORY
operated by
BATTELLE
for the
UNITED STATES DEPARTMENT OF ENERGY
under Contract DE-AC05-76RL01830

Printed in the United States of America

Available to DOE and DOE contractors from the
Office of Scientific and Technical Information,
P.O. Box 62, Oak Ridge, TN 37831-0062;
ph: (865) 576-8401
fax: (865) 576-5728
email: reports@adonis.osti.gov

Available to the public from the National Technical Information Service
5301 Shawnee Rd., Alexandria, VA 22312
ph: (800) 553-NTIS (6847)
email: orders@ntis.gov <http://www.ntis.gov/about/form.aspx>
Online ordering: http://www.ntis.gov


This document was printed on recycled paper.
(8/2010)

PNNL-26924, Rev. 1

NDE Technology Development Program for Non-Visual Volumetric Inspection Technology

Phase I Summary Report

KM Denslow
TL Moran
MR Larche
SW Glass

January 2018

Prepared for
the U.S. Department of Energy
under Contract DE-AC05-76RL01830

Pacific Northwest National Laboratory
Richland, Washington 99352

Preface

This report provides a summary of the outcomes and findings from the sensor testing and evaluation work performed under Phase I of the NDE Technology Development Program during FY2017 and the first quarter of FY2018.

The objective of this Phase I summary report is to provide a condensed version of the information provided in the program plan, Phase I test plans, the two FY2017 test reports issued for *Technology Screening* and *Sensor Effectiveness Testing*, and the test report for FY2018 "Vulnerability" testing. The purpose of the report is to support the selection of sensor technologies for maturation under Phase II of the NDE Technology Development Program.

The full details of the flaw detection test mock-ups and surrogate flaws, sensor technologies, evaluation criteria, and evaluation results are captured between the FY2017 test reports (Moran et al. 2017a, b) and this report.

Acronyms and Abbreviations

ASNT	American Society of Nondestructive Testing
DOE	U.S. Department of Energy
DST	double-shell tank
EMAT	electromagnetic acoustic transducer
NDE	non-destructive evaluation
PNNL	Pacific Northwest National Laboratory
SET	Sensor Effectiveness Testing
SH	shear-horizontal
SNR	signal-to-noise ratio
SV	shear-vertical
SwRI	Southwest Research Institute
WRPS	Washington River Protection Solutions, LLC

Contents

Figures

Tables

Summary

The U.S. Department of Energy (DOE) and the Hanford Site Tank Operations Contractor, Washington River Protection Solutions, LLC (WRPS), are sponsoring a non-destructive evaluation (NDE) technology development program to identify and mature volumetric (non-visual) NDE technology to enable the examination of Hanford double-shell tank (DST) bottoms. NDE technology for Hanford under-tank examination will be made possible through technology maturation that includes sensor adaptation to overcome access challenges presented by tank risers and refractory pad air-slots, followed by integration with robotic delivery systems and ultimately qualification and deployment of the inspection systems. The stages of technology maturation and the testing and evaluation required to support the process are organized under the three program phases summarized in Figure S.1.

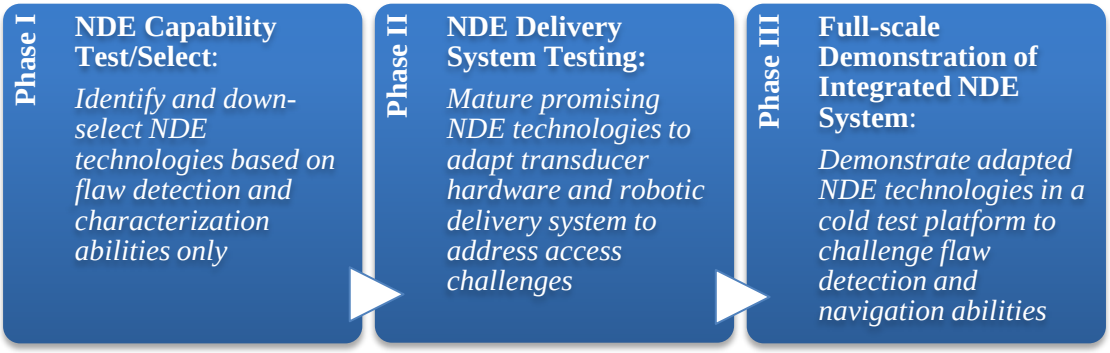

Figure S.1. Summary of the NDE Technology Development Program

Phase I of the program focused on completing the following five key activities:

1. Identifying a broad cross section of potentially applicable NDE volumetric inspection technologies for under-tank examination.
2. Down-selecting the broad set of NDE technologies to a set of strong candidates based on initial flaw detection performance and potential to be adapted/matured to overcome primary tank access challenges posed by access risers and/or refractory pad air-slots.
3. Evaluating the flaw detection performance of the candidate sensors through testing.
4. Using the test results to baseline sensor performance against the flaw detection requirements established for high-level waste tanks.
5. Assessing the trade-offs and vulnerabilities of the candidate sensors that would negatively impact sensor performance reliability or complicate tank inspection operations.

The completion of the first three key activities satisfied the first two Phase I test objectives, which were to complete *Technology Screening* and *Sensor Effectiveness Testing*. Completion of the fourth key activity satisfied the final test objective of Phase I, which was to determine the extent to which the sensors can satisfy high-level waste tank flaw detection requirements. Flaw detection performance results yielded the strengths and weaknesses of each sensor option, which were used to identify strategic combinations of sensor types. The fifth key activity was performed to evaluate sensor risks and challenges for consideration with flaw detection performance.

The Phase I evaluation results will be used to support the Phase I *programmatic objective*, which is to identify one or more NDE sensor technologies for adaptation and maturation for the DST environment.

The selection of one or more sensors will be made by WRPS to mark the culmination of Phase I of the NDE Technology Development Program. The key Phase I outcomes recommended for consideration in the sensor selection process are the following:

1. Sensors that provide an optimal balance between flaw detection requirement satisfaction and risks associated with sensor maturation, deployment, and operation will likely provide the best chance of successfully performing a tank bottom examination under the program's timeline. The scores for flaw detection, sensor attributes, and deployment considerations are provided in Table S.1 along with key benefits and trade-offs.

2. Each sensor option has risks related to sensor maturation or deployment and operation in the tank environment. The risks associated with each sensor option in four leading risk categories are provided in Table S.2. The risks in **bold text** and fully outlined in **bold red** are those that are high risk and *uncontrollable*, or are *controllable* but have a higher risk of failure. The remainder of the risks in the table are considered lower or manageable through reasonable hardware adaptation.

3. Remote examination followed by air-slot examination would support a strategic under-tank inspection plan that entails initially screening the tank bottom remotely to identify potentially flawed regions that would be further investigated by higher-resolution air-slot sensor technology.

As shown in Table S.1, each of the three air-slot sensors scored high in the flaw detection category, with each having successfully detected flaws in over 90% of the flaw scenarios. However, all sensors have risks concentrated in either the sensor maturation phase or the sensor deployment phase that may be important to consider. The highest-risk attributes and trade-offs, which are identified in Table S.2, would either need to be accepted or managed through investment in research/technology development for the air-slot sensor or the robotic deployment system. Only one remote sensor technology was tested and evaluated under Phase I due to the low quantity of available technology options in this category. The remote sensor earned the lowest scores in all three categories; however, it provides an opportunity for strategic rather than random selection of air-slots for the deployment of air-slot sensors.

Table S.1. Summary of Final Weighted Scores for Flaw Detection, Sensor Attributes, and Deployment Trade-offs per Sensor

	Ultrasonic Guided Wave Sensor Option	Total Score	Flaw Detection Subtotal (of 83)	Sensor Attribute Subtotal (of 160)	Deployment Trade-off Subtotal (of 139)	Key Benefits	Key Trade-offs
Air-slot	Single-sensor piezoelectric (Guidedwave)	333	78	144	111	•Single air-slot deployment •Simple image-based analysis •High signal-to-noise ratios	•Low sensitivity to gradual wall thinning •Moderate sensor modification required •Requires 20–50 lb. force applied
Air-slot	Single-sensor EMAT (Innerspec)	320	75	148	97	•Single air-slot deployment •No couplant required	•Significant sensor modification required •Analysis is more difficult (A-scan based)
Air-slot	Dual-sensor EMAT (Penn State)	310	81	142	87	•Sensor size deployment ready •No couplant required	•More intensive deployment; requires two open and adjacent air-slots plus coordinated sensor rotation and translation with high spatial accuracy
Remote	Single-sensor EMAT (SwRI)	290	59	139	92	•No under-tank access required •No couplant required	•Least sensitive to in-weld defects •Not sensitive to gradual wall thinning •Significant sensor modification required to reduce size and weight

Table S.2. Leading Risks Associated with Each Candidate Volumetric NDE Sensor Technology

Leading Risk Category	Dual-Sensor EMAT (Penn State)	Single-Sensor Piezoelectric (Guidedwave)	Single-Sensor EMAT (Innerspec)	Single-Sensor EMAT (SwRI)
Vulnerabilities	The presence of mill scale is expected to impact the ability to reliably detect gradual wall thinning.	Applicable to large plate areas only, approximately 15 ft.^{2} and larger (i.e., the center bottom plates could not be examined with this technique).	**The shear-vertical (SV) wave mode will undergo mode conversion/attenuation in slurry-backed tank plates, which will limit examination range.**	Any obstructions on the lower tank sidewall (e.g., weld brackets, conduit, or ventilation) will preclude examination of that area.
Degree of sensor maturation required to prepare for the operational environment	The sensors are compatible with air-slot sizes and minimal changes would be needed.	**Sensor requires either a dry couplant or liquid couplant to be placed between the sensor face and the test surface to satisfy acoustic impedance matching requirements. A liquid couplant would need to be managed through containment and potentially need to undergo corrosion compatibility testing.**	**Significant sensor down-sizing is required and additional electronics may need to be down-sized and co-deployed with the sensor in the air-slots to manage signal attenuation effects from cables. An experimental multi-layer coil design for the sensor is also proposed to eliminate the need to robotically rotate the sensor inside air-slots.**	**Significant size and weight reduction would be required, which would be accompanied by a high risk of negative impact to sensor performance.**
Impact of motion requirements on the complexity of the robotic delivery system	**Two sensors are used that would require two air-slot robots to be deployed in the same and adjacent air-slots. Rotation and translation routines needed to satisfy the full suite of flaw detection capability must be done in a coordinated fashion with high spatial (0.25 in.) accuracy to support reliable signal processing and flaw detection.**	The sensor must be pressed against the tank bottom regardless of the couplant used. A dry couplant would require a higher force of 20–50 lb. No sensor rotation is required.	The sensor must be rotated inside the air-slots if the multi-layer sensor coil design is not pursued or does not work.	If the weight of the sensor system cannot be reduced to 50–100 pounds, then the robotic delivery system will need to be engineered to bear significant weight. This will be especially important for sensor support if power is lost.
Range	Demonstrated range during testing was 36–48 in., depending on the sensor configuration.	Demonstrated range during testing was 5–7 feet, limited by the test mock-up size.	**Demonstrated range in the presence of a slurry is 6–10 in.**	Demonstrated range during testing was up to 14 ft., limited by the length of the test mock-up.

1.0 Candidate Volumetric NDE Sensor Technologies

Four NDE sensor technologies were evaluated during Phase I that use ultrasonic shear-wave guided-wave techniques to volumetrically examine areas around the sensors that extend over ranges of approximately 6 inches to over 14 feet, depending on the sensor. The ability to examine plate volumes that far exceed the sensor footprints renders ultrasonic guided-wave methods highly valuable for under-tank examination given there are extensive restrictions to direct access to the primary tank bottoms presented by the primary tank refractory pad as shown in Figure 1.

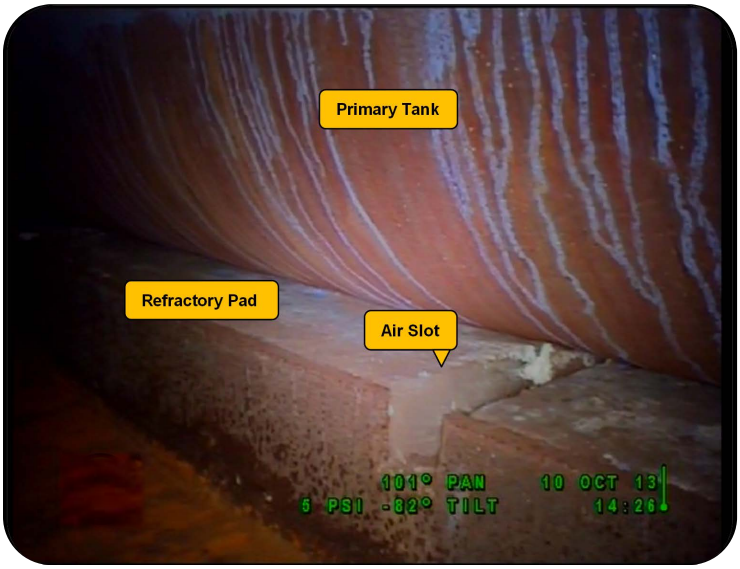

Figure 1. Photograph of a Refractory Pad Air-slot beneath a Primary Tank

The four ultrasonic guided-wave NDE sensor technologies evaluated under Phase I fall into one of two deployment categories: deployment on the primary tank wall for long-range remote examination of the tank bottom (one technology option) or deployment directly on the tank bottom surface exposed by the refractory pad air-slots for short- to medium-range examination of the tank bottom (three technology options).

The following vendors demonstrated the following sensor techniques:

- Southwest Research Institute (SwRI) demonstrated a remote examination electromagnetic acoustic transducer (EMAT) technique for under-tank examination from the primary tank wall.
- Guidedwave demonstrated a single-sensor piezoelectric phased-array technique for air-slot based examinations.
- Innerspec demonstrated the single-sensor EMAT technique for air-slot based examinations.
- Penn State demonstrated a dual-sensor EMAT technique for air-slot based examinations.

Photographs of each of the four sensor techniques are provided in Figure 2. For more detail on each of the technologies, see the *Sensor Effectiveness Testing* report (Moran et al. 2017b).

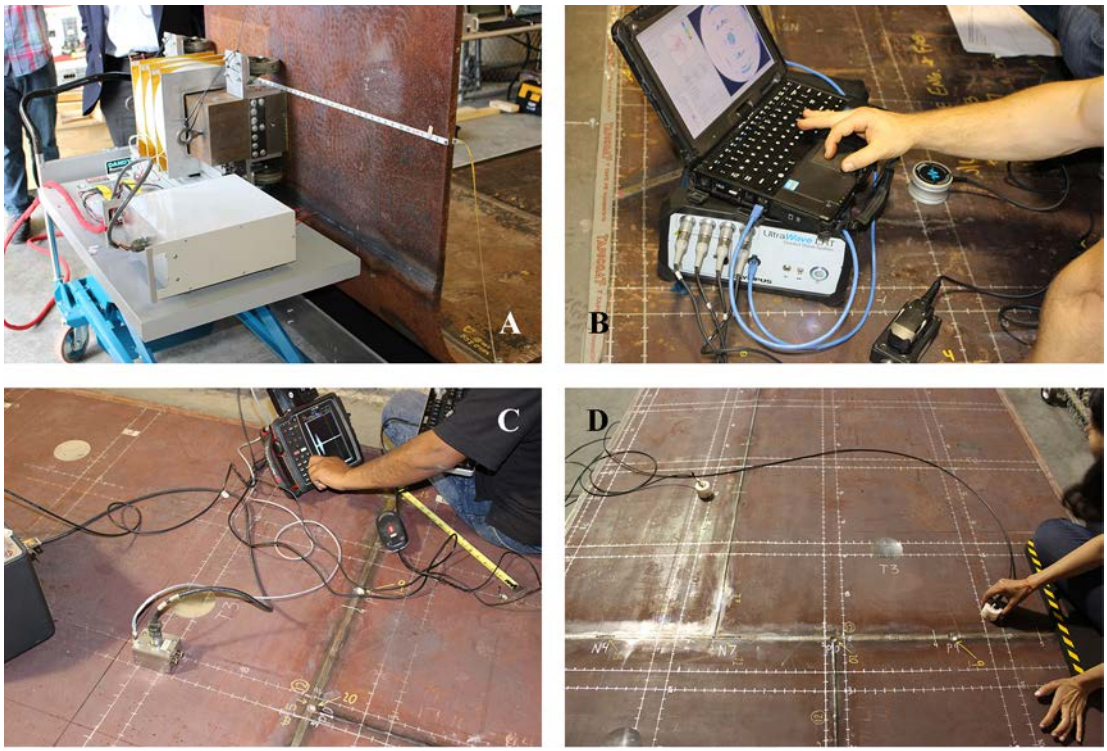

Figure 2. (A) Remote Examination EMAT Technique Demonstrated by SwRI; (B) Air-slot Single-sensor Piezoelectric Phased-array Technique Demonstrated by Guidedwave; (C) Air-slot Single-sensor EMAT Technique Demonstrated by Innerspec; (D) Air-slot Dual-sensor EMAT Technique Demonstrated by Penn State

2.0 Testing and Evaluation

The full scope of Phase I sensor technology testing and evaluation was performed during three separate periods: the official *Technology Screening* and *Sensor Effectiveness Testing* campaigns in FY2017 for all four sensor vendors, an unofficial extended flaw detection test in FY2017 for Penn State, and an official "vulnerability" test in the first quarter of FY2018 for Guidedwave and Innerspec.

FY2017 testing was designed to evaluate the four sensors on flaw detection scenarios and all foreseeable sensor attributes based on high-level waste tank flaw detection requirements and the scope of sensor types and designs. FY2018 testing was designed to evaluate specific sensor attributes ("vulnerabilities") that were introduced during or after FY2017 testing due to changes in sensor type/design features.

This section describes the test setups and conditions used for the test campaigns.

2.1 Sensor Flaw Detection Performance Testing in FY2017

Sensor flaw detection performance was evaluated with testing in a non-nuclear laboratory environment using test mock-ups that represented full-scale swaths of a primary tank. The test mock-ups were constructed with representative carbon steel plate materials, plate geometries and welds, and contained a total of 25 surface-connected surrogate flaws that bounded and included flaw types and sizes that have

been established as the flaw detection requirements for high-level waste tanks (Bandyopadhyay et al. 1997; Boomer et al. 2016). The flaw detection criteria are provided in Table 1.

Table 1. Actionable and Reportable Level Values for High-Level Waste Tanks

Flaw Type	Actionable Level Values	Reportable Level Values
Pit (pitting corrosion)	50% thickness	25% thickness
Crack	> 12 in. length, 20% of thickness < 12 in. length, 50% of thickness	Any linear indication greater than 6 in. in length and 0.1 in. in depth
Wall thinning (general or uniform corrosion)	20% thickness	10% thickness

Photographs of the test mock-ups and examples of surrogate flaws are provided in Figures 3 and 4. The flaws were located in the mock-ups in locations that represent one of the four different potential DST flaw location scenarios listed below. Surrogate wall thinning flaws were located only within the base plate while surrogate pits and weld seam openings were located within the base plate and within or adjacent to welds.

1. 1/2 in. thick mid-floor base plate that comprises approximately 80% of the primary tank bottom area. The plate material is low-carbon carbon steel (ASTM A515, A516, A537) (Boomer et al. 2016).
2. Welds that join 1/2 in. to 1/2 in. thick bottom plates, which are present between all of the mid-floor bottom plates and comprise a majority of the welds in the primary tank bottom. The welds are full penetration butt welds.
3. Transition welds that join 7/8 in. to 1/2 in. thick bottom plates, which are present between the outer bottom plate (7/8 in. thick) and the first mid-floor bottom plate found along the entire tank bottom. The transition weld is the second most common weld in the primary tank bottom and would be the first bottom weld encountered during remote or air-slot based examinations. The transition welds are full penetration butt welds, many of which were re-worked and rendered them representative of re-worked welds in the primary tanks.
4. A tightly spaced confluence of 90-degree welds that join 1/2 in. to 1/2 in. thick bottom plates. The 90-degree weld confluence is located within a region of the 241-AY-102 tank where confirmed leak sites were located (Follett 2017).

   The 90-degree weld confluence is the least common weld found in the primary tank bottoms; however, it may be a tank bottom feature that is at high risk for flaw development if weld stress relieving was not performed adequately during construction. The welds are full penetration butt welds that form a tightly spaced 90-degree weld confluence (pinwheel pattern). The 90-degree weld confluence is found in two to four different locations in the primary tank bottoms of the DSTs located in three of the six tank farms (241-AY, 241-AZ, and 241-SY). The six in-service tanks in the AY, AZ, and SY tank farms represent the oldest of the 27 in-service DSTs at 40–46 years old (Venetz and Gunter 2014).

Figure 3. Photographs of the Full-scale Mock-ups of Swaths of a Primary Tank

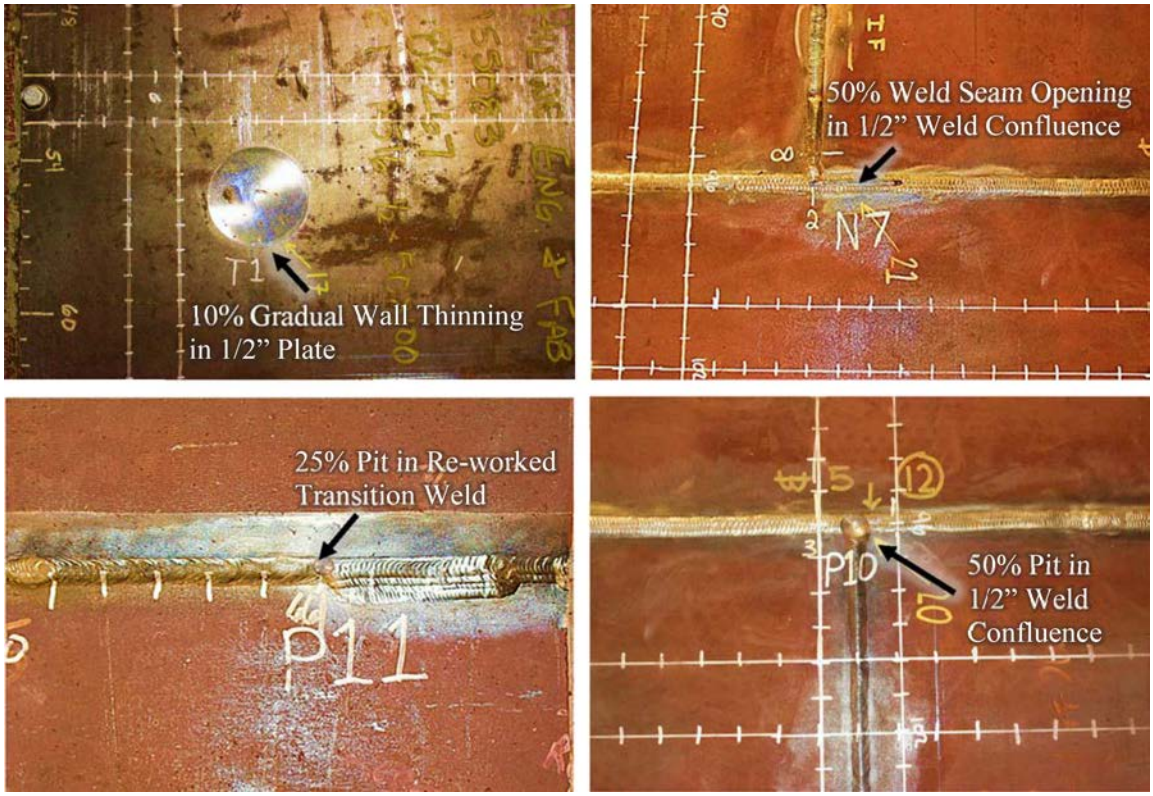

Figure 4. Photographs of Four Examples of Surrogate Flaws

The full set of flaws are described in detail in the *Sensor Effectiveness Testing* report (Moran et al. 2017b).

All flaw detection performance testing was completed by Guidedwave, Innerspec, and SwRI during the official FY2017 test campaigns and most flaw detection performance testing was completed by Penn State during official testing. A limited scope of unofficial testing was conducted by Penn State after official FY2017 testing had concluded in June 2017 to allow the university team an opportunity to collect data on two flaws they had neglected to scan during official testing. On August 1, 2017, Penn State returned to PNNL to acquire data on the 10% wall thinning flaw (Flaw T1) and the 50% notch located in

the 90-degree weld confluence (Flaw N7). All of the same instruments and settings were used as those used in the *Sensor Effectiveness Testing* conducted in June 2017.

2.2 Sensor Attribute "Vulnerability" Testing in FY2018

To support the final sensor selection process, the risks and challenges related to sensor attributes and deployment trade-offs were evaluated and scored to identify the sensors that can provide optimal balance between flaw detection requirement satisfaction and practicality of sensor maturation and deployment. All foreseeable sensor attributes and deployment trade-offs were evaluated during FY2017 and any attributes related to measurement physics were addressed with testing during the course of flaw detection performance testing.

However, concerns about unforeseeable sensor attributes emerged for the shear-vertical (SV) EMAT (Innerspec) when the sensor type changed during the course of testing, and the piezoelectric phased-array sensor (Guidedwave) when the sensor couplant feature changed after the conclusion of testing. For the SV electromagnetic acoustic transducer demonstrated by Innerspec, the concern was the extent to which the examination range and signal quality of the new ultrasonic SV wave mode would be impacted when a slurry was in contact with the test surface. For the piezoelectric phased-array sensor demonstrated by Guidedwave, the concern was the impact a dry couplant material would have on sensor signal quality and thus flaw detection performance if used in place of the viscous shear liquid coupling that was initially demonstrated.

The two specific concerns were related to sensor measurement physics and therefore could be addressed by conducting a simple demonstration. The demonstration took place in the first quarter of FY2018 at the November 2017 American Society of Nondestructive Testing (ASNT) annual meeting in Nashville, Tennessee. This section describes the test mock-up, test conditions, and testing in detail because a separate interim test report was not issued for the testing conducted in Nashville.

The EMAT sensor technologies demonstrated by Penn State and SwRI in FY2017 have leading risks that are not related to the underpinning measurement physics of these two sensors. Therefore, additional testing of these EMAT sensors before maturation would not have provided results that are valuable to the sensor selection process and, thereby, Penn State and SwRI EMAT sensors were excused from the demonstration.

2.2.1 Test Plate and Surrogate Flaws

The test plate used for sensor attribute vulnerability testing was a flat, A36 carbon steel plate that was 24 in. × 48 in. × 0.5 in. and contained two surrogate pits on one side of the plate. Details on the plate size and pit size and location are provided in Figure 5 and Table 2. The surface condition of the plate was the natural state of the as-received carbon steel plate. The surface condition and surrogate pit size and placement were no more challenging than that which was presented during FY2017 *Sensor Effectiveness Testing*.

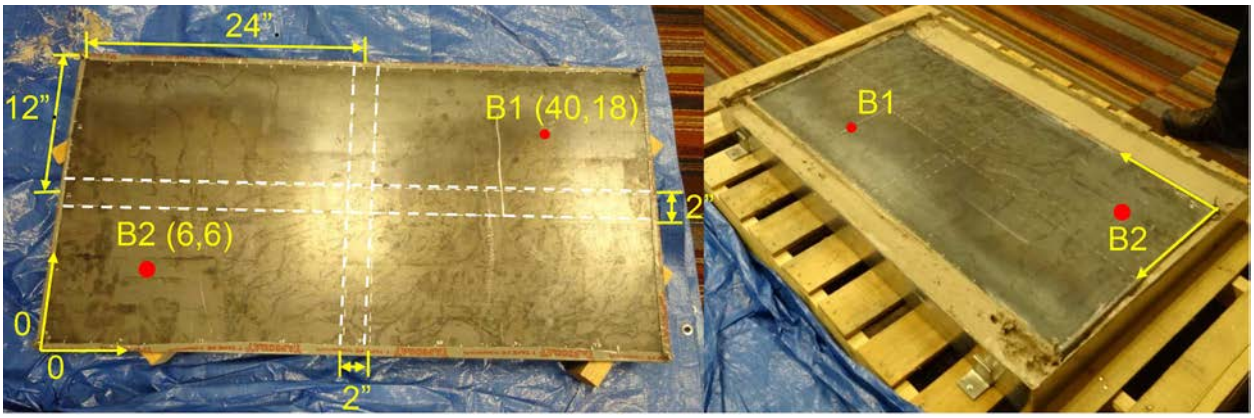

Figure 5. Pictures of the Carbon Steel Test Plate Used for Sensor Attribute Vulnerability Testing in Nashville, Tennessee: (a) shows locations of the two blind pits (red dots) and (b) shows the plate that is in the kaolin clay slurry mixture.

Table 2. Surrogate Flaws to Support Post-Sensor Effectiveness Testing

Machined Surrogate Flaw	Flaw Depth[(a)]	Diameter	Flaw ID	Flaw Location and Orientation in Mock-up
Pit	25% t, 0.125 in.	0.375 in.	B1	(40 in., 18 in. from origin), bottom of base plate
Pit	50% t, 0.25 in.	0.75 in.	B2	(6 in., 6 in. from origin), bottom of base plate

t = plate thickness

2.2.2 Test Conditions

The format of the demonstration was a "blind" test; i.e., the flaw type, sizes, and locations were not disclosed outside the project team prior to testing. The flawed side of the test plate was placed face down while in contact with air ("air-backed") or the test slurry ("slurry-backed") so the flaws were not visible during the demonstration. The participants were asked to leave the room while the plate was handled.

The slurry used was a kaolin and water mixture (density is 1.65 g/cc) that is non-hazardous and simulates the acoustic impedance and attenuation of waste located at the bottom of Hanford high-level waste tanks. The slurry was contained in a shallow basin that was filled to a level of approximately 4 in. While inside the basin, the plate was supported at all four corners by pegs that were approximately 1 in. dia. While outside the basin, the plate was supported at all four corners by wood 2×4 blocks that provided a 4 in. separation between the plate and the floor.

Each participant performed their demonstration separately using the same sensors that were used during FY2017 *Sensor Effectiveness Testing*. The sensors were placed on the broadside of the test plate opposite the flawed side of the plate during the demonstration. The participants were allowed to perform scoping measurements from any position on the plate; however, it was required that reportable data be recorded from the designated 2 in. wide virtual air-slots marked along the center of each axis of the plate as shown in Figure 5.

2.2.3 Testing

The objective of the demonstration for Innerspec was to observe and quantify the extent to which the flaw detection range and signal quality of the 2.25 MHz SV wave EMAT was impacted when slurry is in contact with the test plate (see Figure 6). The demonstration was conducted from the two virtual air-slots, which created a minimum distance between sensor and flaws of 6 in. for the long axial air-slot and minimum distances of 16 in. or 18 in. for the lateral air-slot.

Innerspec inspected the air-backed plate first. Their inspection approach involved placing the sensor in a virtual air-slot and performing a continuous scan from one edge of the plate to the other. When an indication was detected, they marked the locations with tape and went back to the discrete locations after the continuous scan to record reportable data. Detection of the flaws from the slurry-backed plate was attempted from the same sensor locations using the same settings to facilitate a direct comparison of the signals. Additional measurements with other instrument settings were permitted after measurements with the same settings were performed.

Figure 6. EMAT Technique Using Shear Vertical Sensor on Air- (*left*) and Slurry-backed (*right*) Test Plate

The objective of the demonstration for Guidedwave was to observe and quantify the extent to which the flaw detection performance of the 165 kHz SH wave piezoelectric phased-array sensor was impacted when a dry couplant is used in lieu of the standard liquid shear couplant. The negligible impact of the slurry on the signal that was expected was also tested. The demonstration was conducted by requesting Guidedwave to collect data on the air-backed and slurry-backed test plate using their new dry shear-wave couplant and the traditional liquid shear-wave couplant. The same sensor positions and instrument settings were used for each combination to facilitate a direct comparison of the signals.

The dry-coupling method is a newly developed proprietary coupling method that would eliminate the need for couplant dispensing, application, or cleanup during remote testing on the DSTs. To obtain the proper amount of surface coupling with the dry couplant, a 50 lb. calibration weight was placed on top of the probe during the demonstration as shown in Figure 7(a). After each measurement, the weight was removed and the probe with dry coupling was easily removed and placed in the next position. Measurements were collected from the center of the test plate as shown in Figure 7(b) as well as along the axial virtual air-slot. No force was applied to the sensor during data collection with the liquid couplant.

Guidedwave inspected the slurry-backed test plate first and then the clean air-backed plate with both the new dry shear-wave couplant and the traditional shear-wave liquid couplant. The slurry was thoroughly cleaned from the test plate before the air-backed measurements were collected (see Figure 8). The

inspection approach involved placing the sensor at the center location of the plate at the intersection of both virtual air-slots and performing a 360-degree scan through electronic beam steering (not sensor rotation). After completing the first scan, the sensor was moved to the next location 6 in. away. The process was repeated in 6 in. increments along both air-slots from the same sensor locations for the slurry-backed and air-backed test plate. Three data sets collected from sensor positions furthest from the plate edges were averaged [(18, 12), (24, 12), and (30, 12)] and used to report flaw locations and SNR values.

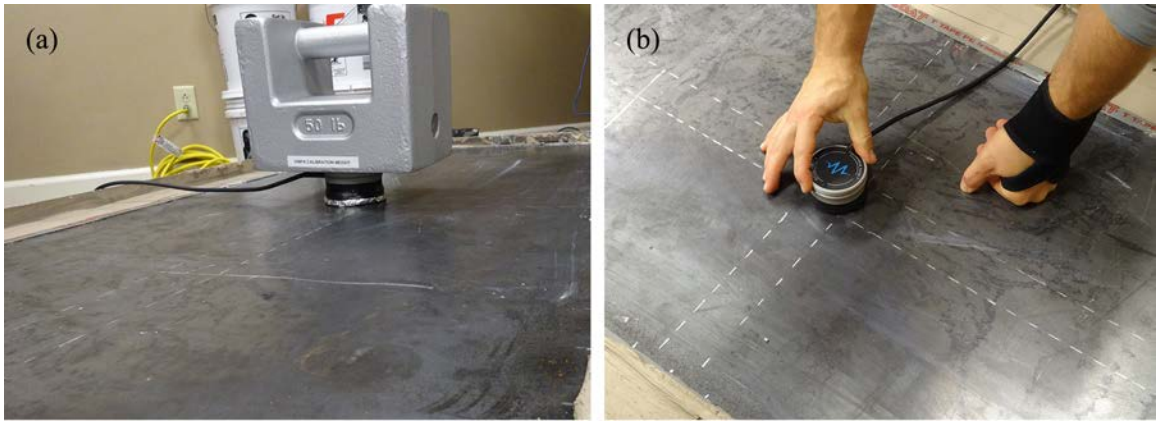

Figure 7. Piezoelectric Phased-array Technique (a) Dry Coupling Technique with a 50 lb. Weight, and (b) Liquid Coupling Technique in Direct Contact with Test Surface

Figure 8. Bottom of the Test Plate after Removing the Slurry, Revealing the Two Locations of the Pits

3.0 Sensor Technology Evaluation

The Phase I flaw detection performance test results were used to satisfy the final test objective of Phase I, which was to determine the extent to which the sensors can satisfy high-level waste tank flaw detection requirements. The sensor risks and challenges were also evaluated to uncover the most significant strengths, weaknesses, and risks associated with each sensor option.

This section provides the results of the flaw detection performance evaluation and the sensor attribute and deployment trade-off evaluation that together can be used to identify sensors that can provide an optimal balance between flaw detection requirement satisfaction and practicality of sensor maturation and deployment. The results from the full scope of Phase I testing and evaluation conducted over three

separate periods in FY2017 and FY2018 are included. The criteria used for the flaw detection performance, sensor attribute, and deployment trade-off evaluation are captured in the FY2017 *Sensor Effectiveness Testing* report (Moran et al. 2017b).

3.1 Evaluation of Flaw Detection Performance

The extent of flaw detection requirement satisfaction was quantified per sensor using a summation of points awarded for each of the 25 flaws detected during FY2017 flaw detection performance testing.[(a)] In Table 3 are the original flaw detection scores from official *Sensor Effectiveness Testing* (SET) and the updated scores (post-SET) after incorporating the results of extended flaw detection testing described below in Section 3.1.1. The only flaw detection score affected by extended testing was that of Penn State.

The rolled-up flaw detection subtotals for each sensor are good indicators of individual sensor flaw detection performance and are useful for comparing relative performance. For instance, the flaw detection scores reveal that the three sensors for air-slot deployment satisfy high-level waste tank flaw detection requirements to a much greater extent than the remote examination sensor technology.

However, the rolled-up flaw detection scores do not indicate the sensitivity each sensor has to each flaw type (i.e., flaw detection strengths and weaknesses). To assess flaw detection strengths and weaknesses and to uncover technologies that provide the greatest extent of flaw detection requirement satisfaction, the aggregate set of flaw detection test results for the four sensor technologies were mapped onto a composite FY2017 test plan flaw matrix. The flaw matrix includes results from the two FY2017 test campaigns and is organized by flaw type and size under the four different previously listed potential flaw location scenarios in Section 2.1.

The results of the mapping are provided in Table 4. The colored cells in Table 4 indicate the flaw types, sizes, and potential flaw location scenarios that were included in the scope of Phase I testing between *Sensor Effectiveness Testing* and *Technology Screening*. For convenience, the yellow-highlighted cells indicate flaws included in *Sensor Effectiveness Testing*, the blue-highlighted cells indicate flaws included in *Technology Screening*, and the green-highlighted cells indicate flaws included in both test campaigns. The flaw detection requirements are noted in the cells along with the specific sensor technologies that succeeded in flaw detection under each flaw scenario. A “Yes” means a detection occurred above the minimum SNR 6 dB or 2:1 ratio and a “No” means no detection.

The success claims for each sensor technology are based on the results of *Sensor Effectiveness Testing* and *Technology Screening*. Comparing the results across the two campaigns is reliable for three vendors whose sensor technologies were consistent across both campaigns (Guidedwave, Penn State, and SwRI). The fourth vendor changed sensor technologies between *Technology Screening* and *Sensor Effectiveness Testing* and, as a result, only comparing the results across the yellow- and green-highlighted cells is reliable for this vendor. In the event there were conflicting answers from vendors for the subset of flaws included under both test campaigns (green-highlighted cells), the results from the advanced *Sensor Effectiveness Testing* superseded the results from the preliminary *Technology Screening* tests because either the sensors or the sensor configuration for *Sensor Effectiveness Testing* were considered optimized.

(a) Flaw detection results for the nine flaws from the preliminary *Technology Screening* are not included in Table 3 with flaw detection results for the 25 flaws from *Sensor Effectiveness Testing* because one of the four vendors changed sensor technologies during *Sensor Effectiveness Testing*, which rendered comparison of the performance of two different sensor technologies unreliable for that vendor.

Table 3. Summary of Raw Scores for Flaw Detection, Sensor Attributes, and Deployment Trade-offs per Sensor

	Ultrasonic Guided Wave Sensor Option	Flaw Detection Subtotal (of 83)		Sensor Attribute Subtotal (of 50)		Deployment Trade-off Subtotal (of 41)		Key Benefits	Key Trade-offs
		SET	**Post-SET**[(a)]	SET	**Post-SET**[(b)]	SET	**Post-SET**[(a,c)]		
Air-slot	Single-sensor piezoelectric (Guidedwave)	78	**78**	42	**43**	30	**30**	•Single air-slot deployment •Simple image-based analysis •High signal-to-noise ratios	•Low sensitivity to wall thinning •Moderate sensor modification required •Applicable to large plate areas only, approximately 15 ft^2 and larger (i.e., the center bottom plates could not be examined with this technique)
Air-slot	Dual-sensor EMAT (Penn State)	73	**81**	44	**44**	26	**27**	•Sensor size deployment ready •No couplant required	•More intensive deployment; requires two open and adjacent air-slots plus coordinated sensor rotation and translation with high spatial accuracy
Air-slot	Single-sensor EMAT (Innerspec)	75	**75**	42	**42**	28	**27**	•Single air-slot deployment •No couplant required	•Significant sensor modification required •Analysis is more difficult (A-scan based)
Remote	Single-sensor EMAT (SwRI)	59	**59**	41	**41**	26	**26**	•No under-tank access required •No couplant required	•Least sensitive to in-weld defects •Not sensitive to wall thinning •Significant sensor modification required to reduce size and weight

(a) During *Sensor Effectiveness Testing*, Penn State did not report on the 10% wall thinning flaw (Flaw T1) or the 50% notch located in the 90-degree weld confluence (Flaw N7) due to failure to record the data at the time of testing. After *Sensor Effectiveness Testing*, Penn State acquired additional data on Flaws T1 and N7 using the same instrumentation and settings used previously and was able to detect both flaws. Penn State provided the results in a test report that is discussed in Appendix A of this report.

(b) During *Sensor Effectiveness Testing*, Guidedwave was using a "wet" shear couplant that required couplant to be applied remotely and actively removed by scrubbing. During the sensor attribute "vulnerability" demonstration in Nashville, Guidedwave demonstrated a dry couplant. Guidedwave provided the results from the demonstrations in a report that is discussed in Appendices B and D of this report.

(c) The wall thinning score for both Penn State and Innerspec should have both been a value of 3 during *Sensor Effectiveness Testing* since they were only able to detect the actionable level thinning (20%). After *Sensor Effectiveness Testing*, Penn State was able to demonstrate the detection of the 10% wall thinning flaw (Flaw T1).

Table 4. Mapping of Phase I Test Results onto the Phase I Test Plan Flaw Matrix. Colored cells indicate the flaw types and sizes included in the scope of Phase I testing, yellow-highlighted cells indicate flaws included in *Sensor Effectiveness Testing*, blue-highlighted cells indicate flaws included in *Technology Screening*, and green-highlighted cells indicate flaws included in both test campaigns. No = not detected. Yes = detected.

	Depth (% Plate Thickness)	Pit		Wall Thinning		Axially Oriented Notch[a]		Circumferentially Oriented Notch[a]	
		Remote	**Air-slot**	**Remote**	**Air-slot**	**Remote**	**Air-slot**	**Remote**	**Air-slot**
1/2 in. Base Plate	10%			*Reportable Level*					
				No	Yes-PS[d]				
	20%			*Actionable Level*		*Reportable Level*[b]		*Reportable Level*[b]	
				No	Yes-PS, IS[c]			Yes-SwRI	Yes-PS, GW, IS[c]
	25%	*Reportable Level*							
		Yes-SwRI	Yes-PS, GW, IS[c]						
	50%	*Actionable Level*		**No**	Yes-PS, GW, IS[c]	*Actionable Level*		*Actionable Level*	
		Yes-SwRI	Yes-PS, GW, IS[c]			**No**	Yes-PS, GW, IS[c]	Yes-SwRI	Yes-GW, IS[c]
	75%	Yes-SwRI	Yes-PS, GW, IS[c]						
	90%	Yes-SwRI	Yes-PS, GW, IS[c]			Yes-SwRI	Yes-PS, GW, IS[c]		
	100% (hole)	Yes-SwRI	Yes-PS, GW, IS[c]						

	Depth (% Plate Thickness)	Pit		Axially Oriented Notch[a]		Circumferentially Oriented Notch[a]	
		Remote	**Air-slot**	**Remote**	**Air-slot**	**Remote**	**Air-slot**
1/2 in. Plate –to-1/2”Plate Straight Welds	20%			*Reportable Level*[b] Yes-SwRI	Yes-PS, GW, IS[c]	*Reportable Level*[b]	
	25%	*Reportable Level* Yes-SwRI	Yes-PS, GW, IS[c]				
	50%	*Actionable Level* Yes-SwRI	Yes-PS, GW, IS[c]	*Actionable Level* Yes-SwRI	Yes-PS, GW, IS[c]	*Actionable Level* Yes-SwRI	Yes-PS, GW, IS[c]
	75%	**No**	Yes-PS, GW, IS[c]				
	Depth (% Plate Thickness)	**Pit**		**Axially Oriented Notch[a]**		**Circumferentially Oriented Notch[a]**	
		Remote	**Air-slot**	**Remote**	**Air-slot**	**Remote**	**Air-slot**
7/8 in. Plate-to-1/2 in. Plate Straight Transition Weld	20%			*Reportable Level*[b]		*Reportable Level*[b]	
	25%	*Reportable Level* Yes-SwRI	Yes-PS, GW				
	50%	*Actionable Level* Yes-SwRI	Yes-PS, GW, IS[c]	*Actionable Level* Yes-SwRI	Yes-PS, GW, IS[c]	*Actionable Level* **No**	Yes-PS, GW, IS[c]
	75%	Yes-SwRI	Yes-PS, GW, IS[c]				

	Depth (% Plate Thickness)	Pit		Circumferentially Oriented Notch[a]	
		Remote	**Air-slot**	**Remote**	**Air-slot**
1/2 in. Plate-to-1/2 in. Plate 90-degree Weld Confluence	20%	*Reportable Level*		*Reportable Level*[b]	
	25%				
	50%	*Actionable Level*		*Actionable Level*	
		No	Yes-GW, PS, IS[c]	**No**	Yes-GW, IS[c], PS[d]

(a) Criteria for cracks were applied to the notches.

(b) A 20% through-wall crack specified for the actionable level value is equivalent to the 0.1 in. through-wall depth specified for the reportable level value when flaw length is not a factor.

(c) During *Technology Screening*, Innerspec primarily used the magnetostrictively coupled SH wave EMAT technique, not the SV wave EMAT technique used during *Sensor Effectiveness Testing*.

(d) During *Sensor Effectiveness Testing*, Penn State did not report on the 10% wall thinning, T1, and the 50% notch located in the 90-degree weld confluence, N7, due to failure to record the data at the time of testing. After *Sensor Effectiveness Testing*, Penn State acquired additional data on T1 and N7 using the same instrumentation and settings used previously and was able to detect both T1 and N7. Penn State provided the results in a report that is discussed in Section 4 and Appendix A of this report.

The mapping exercise revealed the following four important strengths and weaknesses of the candidate sensor technologies:

1. The three air-slot examination sensor technology options are sensitive to all flaw types in the four different potential flaw location scenarios that were tested. The detection of each flaw type at the actionable level was successfully demonstrated by the single-sensor EMAT technique from Innerspec.
2. The difference in the flaw detection scores for the two higher-scoring air-slot technology options came down to gradual wall thinning and the "blind" pit flaw. The dual-sensor EMAT technology demonstrated by Penn State was sensitive to gradual wall thinning at the reportable and actionable level values; however, the blind pit flaw was missed during testing. The piezoelectric phased-array technology demonstrated by Guidedwave was insensitive to gradual wall thinning at the reportable and actionable level values; however, the technique detected the blind pit flaw.
3. The remote examination sensor technology option is sensitive to surrogate pits in base plate and straight welds and sensitive to surrogate weld seam openings in straight welds.
4. The gaps that exist between the abilities of today's candidate NDE technology and the high-level waste tank flaw detection requirements/flaw location scenarios are: remote sensor detection of wall thinning at any level and remote detection of any flaws located in the 90-degree weld confluence. The impact of these gaps is considered low and can be risk-mitigated with targeted examinations of specific tank regions using air-slot transducers, and development of supplementary remote examination NDE techniques under a separate project with a timescale that is conducive to technology development.

3.1.1 Extended Flaw Detection Performance Test Results for Penn State

Included in the Flaw Detection post-SET scores in Table 3 and the flaw mapping in Table 4 are the results of extended flaw detection performance testing afforded to Penn State. During the extended FY2017 flaw detection performance testing, Penn State detected the 10% wall thinning flaw (Flaw T1) using the through-transmission mode and moving the transmitter and receiver in parallel in 1 in. increments. After reviewing the data, the detection was made evident by a loss of the SH1 mode signal. The signal-to-noise ratio (SNR) was reported as 7 dB. Penn State also detected the notch in the weld confluence (Flaw N7) using the pitch-catch mode with the transmitter and receiver rotated towards each other at 45-degree angles relative to their centerline. The transmitter was at a fixed location and the receiver was moved past the transmitter in 1 in. increments. After synthetic aperture focusing technique (SAFT) post-processing of the data, an image was reconstructed and Flaw N7 was detected with an SNR of 15 dB. For more information on the testing conducted, see Appendix A.

3.2 Evaluation of Sensor Maturation and Deployment Risks

To assess the practicality and risks associated with future sensor maturation and deployment, the four sensor options were assigned scores for sensor attributes and deployment considerations that could negatively impact sensor performance reliability or work intensity during tank inspection operations. The purpose of the exercise was to provide a well-rounded evaluation of each sensor option.

In Table 3 are the original sensor attribute and deployment trade-off scores from official SET and the updated (Post-SET) scores after incorporating the results of "vulnerability" testing described below in Section 3.2.1. The total scores are intended to reflect the degree of balance provided by each sensor

between flaw detection requirement satisfaction and risk associated with sensor maturation and deployment.

Sixteen different risk categories related to sensor maturation and deployment were evaluated under Phase I. Of the 16 categories, the 4 that are perceived to be the leading risk categories are provided in Table 4. Under each of the four categories in Table 4 are the specific risks associated with each sensor technology option. The risks in **bold text** and fully outlined in **bold red** are those that are high risk and uncontrollable, or are controllable but have a higher risk of failure. The remainder of the risks are considered lower or manageable through reasonable hardware adaptation. The leading risks associated with each of the four sensor technology options that should be strongly considered along with flaw detection performance in the sensor selection process are:

- The hardship that would be imposed to deploy the two EMAT sensors demonstrated by Penn State for use in the air-slots should be strongly considered. The two sensors would need to be translated and rotated with high spatial accuracy in a synchronized/coordinated fashion within the same or adjacent air-slots to produce reliable synthetic aperture focusing technique processing results. These sensor requirements will require a sophisticated robotic delivery system and a sophisticated cable management system.
- The reduced examination range of the single-sensor EMAT approach demonstrated by Innerspec for use in the air-slots should be strongly considered. The SV wave mode employed by the technique will undergo mode conversion/attenuation when a slurry is present on the opposite side of the test surface (tank bottom), which will reduce the examination range. For example, the detection range for a pit was reduced from 18 in. during dry testing to 6–10 in. during slurry-backed testing when the same sensor and instrument settings were used. The sensor also requires significant down-sizing, may require pre-amplifier electronics to be co-deployed with the sensor in the air-slots, and may rely on an experimental multi-coil sensor design that has not yet been attempted in order to avoid requiring sensor rotation inside the air-slots.
- The hardship that would be imposed to satisfy the coupling pressure requirement of the single-sensor piezoelectric phased-array technique demonstrated by Guidedwave for use in the air-slots should be strongly considered. The robustness of the dry couplant material needs to be evaluated and the possibility of supplying 20–50 lb. pressure to the sensor by a robotic delivery system should be determined early.
- The extent to which the remote examination EMAT sensors demonstrated by Southwest Research Institute would need to be downsized is the greatest among the four sensors evaluated. The weight of the sensor system may need to be reduced by a factor of 5–10 in order to reach a weight that a reasonable robotic delivery system could accommodate. The risk that sensor downsizing may have on sensor performance should be strongly considered along with the risk of increasing robotic delivery system complexity if the sensor weight cannot be reduced by a factor of 5–10 while preserving/improving the sensor performance demonstrated during testing.

3.2.1 Sensor Attribute “Vulnerability” Test Results for Innerspec and Guidedwave

Included in the Sensor Attribute and Deployment Trade-off scores in Table 3 and the leading risks in Table 4 are the results of the sensor attribute “vulnerability” tests described in Section 2.2. This section provides detailed results of the vulnerability tests because a separate interim test report was not issued.

3.2.1.1 Innerspec Results

Innerspec reported detection of the two flaws in the test plate – one at (6 in., 6 in.) and one at (40 in., 18 in.), which were the true locations of blind flaws B2 and B1, respectively, as shown in Table 5. For the reportable data, the sensor was placed in the axial virtual air-slot at the shortest distance between the flaws and the sensor, which was 6 in. for both B1 and B2. The SNR for each flaws is provided in Table 5.

Innerspec attempted to detect both flaws from the short lateral air-slot of the air-backed plate. The sensor was placed in the virtual lateral air-slot at the shortest distance between the flaws and the sensor, which was 16 in. for flaw B1 and 18 in. for flaw B2. Innerspec was unable to detect either of the defects from the lateral air-slot. The signals for each of the defects at the 16 in. and 18 in. distances were equivalent to the noise level. Innerspec placed their sensor outside the virtual air-slots to determine the distance at which the flaws could be detected. The demonstrated position at which the flaw responses were at least twice the noise level (SNR=2) was approximately 10 in. from the sensor. The distance limitation was observed by Pacific Northwest National Laboratory (PNNL) test supervisors, but not documented in Innerspec's test report.

The SNR values for the SV-EMAT flaw responses for the air-backed and slurry-backed plate are provided in Table 5 along with the signal attenuation for the air-backed and slurry-backed plate. The slurry ultimately resulted in a loss of −6 and −9.2 dB (a factor of 2–3 in signal reduction) over a 6 in. distance. Innerspec's test report is included as Appendix C.

Table 5. SNR Values for the Blind Flaws Detected for Air-backed and Slurry-backed Scenarios

Flaw ID	Distance from Sensor (in.)	Air-backed (dB)	Slurry-backed (dB)	Attenuation due to Slurry-backed Plate (dB)
B1	6	17.1	11.1	−6.0
B2	6	22.4	13.2	−9.2

3.2.1.2 Guidedwave Results

Guidedwave also reported detection of two flaws—one at (6 in., 6 in.) and one at (42 in., 18 in.). The indication reported at (6 in., 6 in.) is the location of blind flaw B2 and the indication reported at (42 in., 18in.) is within 2 in. of the location of blind flaw B1, which is acceptable uncertainty.

Because the test plate geometry ultimately precluded the use of suppression filtering and resulted in lower SNR values for the flaws, Guidedwave opted to use SNR values for the plate edge reflections to support comparisons of signal quality for dry couplant versus liquid couplant and the slurry-backed verses air-backed plate. The average SNR values for the edge reflections are provided in Table 6. A comparison between data sets acquired with the dry couplant and the liquid couplant on the air-backed plate using the same instrument settings shows a difference of 0.2 dB, with the dry-coupling signal quality being slightly higher. The small difference in SNR demonstrates the dry couplant is an acceptable alternative to liquid couplant provided a 50 lb. force is applied to the back of the sensor.

The slurry was expected to have little effect on the signals since the Guidedwave technique uses the SH wave mode, which is non-dispersive and thus theoretically insensitive to liquid in contact with the test surface. A comparison between data sets acquired with the liquid couplant on the slurry-backed and air-backed plate using the same instrument settings shows a difference of 1.2 dB, with the SNR for the

slurry-backed plate being lower. The small reduction in SNR for the slurry-backed plate demonstrates there is minimal, but not zero, energy loss to the SH wave mode with a slurry-backed surface. Guidedwave's test report is included as Appendix D.

Table 6. SNR Values for Plate Edge Reflections and Comparisons between Wet and Dry Coupling

		SNR (dB)				
		Air-backed (Average from 3 locations)		Slurry-backed (Average from 3 locations)		Comparison between Dry and Wet Coupling
Edge Reflection	Distance from Sensor (in.)	Dry	Wet	Dry	Wet	
Average from all Four Sides	6–18	44.7	44.5	N/A	43.3	0.2

3.2.1.3 Discussion

The objective of the demonstration for Innerspec's SV-EMAT sensor was to understand the extent to which mode conversion/attenuation induced by a representative slurry impacts the sensor's measurement range and signal quality, which was identified as a leading risk in FY2017. The impact of the slurry on the signal was evident in the factor of 2–3 signal reduction observed and measured, and is most likely dependent on the flaw size. The signal reduction limited the measurement range to approximately half that observed during dry testing in FY2017. Innerspec successfully detected and correctly located both flaws in the air-backed and slurry-backed plate scenarios when the sensor was located in the axial air-slot position 6 in. away from the flaws; however, the flaws could not be detected in the slurry-backed plate when the sensor was located in the lateral air-slot positions 16–18 in. from the flaws. The maximum distance from the flaws at which flaw response signals could be observed was 10 in. Innerspec believes the measurement range could be increased to a distance of 24 in. or more with sensor aperture widening, more instrument gain, and a distance amplitude correction curve.

Based on the test results, Innerspec has demonstrated the ability to confidently detect flaws located within a 6 in. range using the current sensor design, provided the sensor can be rotated. A 6 in. measurement range would allow for partial, but not complete, examination of tank bottom regions between air-slots. The other leading risk associated with the Innerspec sensor is the need to rotate the sensor robotically or the need to develop an undemonstrated multi-coil design that would remove the need to rotate the sensor. Primary risks to be understood before selecting this sensor option are the reduced range of the sensor and the ability to either rotate the sensor or develop a multi-coil sensor (precluding the need for sensor rotation).

The primary objective of the demonstration for Guidedwave's piezoelectric phased-array sensor was to understand the impact a dry couplant has on signal quality as compared with signals obtained with traditional liquid couplant. Guidedwave encountered two challenges during the demonstration. Although the flaws were located at sufficient distances from the test plate edges to allow for signal resolution, the short length and width of the test plate resulted in several edge reflections that challenged the instrument's suppression filtering that is used to remove such measurement artifacts. When the suppression filtering was applied to reduce edge reflections in the signals, the SNR values for the flaws were also significantly lowered. Although this would not be an issue in the larger test mock-ups or a real tank, it was an artifact of the test that forced Guidedwave to perform data analysis without suppression filtering. As a result, SNR values for the flaws were lower than those observed during FY2017 testing and plate edge

reflections that are normally filtered out were present in the composite images with the flaw responses for the demonstration.

The second challenge was damage to a dry couplant that had been installed onto the sensor prior to shipping. The damage to the dry couplant was realized after data had been collected on the slurry-backed plate and the data set was deemed invalid. The damaged dry couplant was replaced prior to the collection of data on the air-backed plate; however, measurements on the slurry-backed plate to support the secondary test objective (evaluating slurry impact) were not re-collected. The dry-coupled measurements on the slurry-backed plate were not essential to meeting the secondary objective. Both test objectives were met using the liquid-couplant measurements on the slurry-backed plate and the dry- and liquid-couplant measurements on the air-backed plate.

Despite the two challenges, Guidedwave successfully detected the two blind flaws using the new dry-coupling method as well as with the traditional liquid couplant. Guidedwave was also able to demonstrate the results from the dry couplant are comparable to those of the liquid couplant provided a 50 lb. force is applied to the back of the sensor. The comparison between measurements performed on a slurry-backed and air-backed plate demonstrated little impact on the signal by the slurry. The dry couplant has been demonstrated to be an appropriate alternative to traditional liquid couplant and addresses the leading risk that was identified for this sensor. Primary risks to be understood before selecting this sensor option are the ability to obtain an adequate application force required for using the dry couplant, and along with that the robustness of the dry couplant surface.

Table 7. Leading Risks Associated with each Candidate Volumetric NDE Sensor Technology

Leading Risk Category	Dual-Sensor EMAT (Penn State)	Single-Sensor Piezoelectric (Guidedwave)	Single-Sensor EMAT (Innerspec)	Single-Sensor EMAT (SwRI)
Vulnerabilities	The presence of mill scale is expected to impact the ability to reliably detect gradual wall thinning.	Applicable to large plate areas only, approximately 15 ft.^{2} and larger (i.e., the center bottom plates could not be examined with this technique).	**The shear-vertical (SV) wave mode will undergo mode conversion/attenuation in slurry-backed tank plates, which will limit examination range.**	Any obstructions on the lower tank sidewall (e.g., weld brackets, conduit, or ventilation) will preclude examination of that area.
Degree of sensor maturation required to prepare for the operational environment	The sensors are compatible with air-slot sizes and minimal changes would be needed.	**Sensor requires either a dry couplant or liquid couplant to be placed between the sensor face and the test surface to satisfy acoustic impedance matching requirements. A liquid couplant would need to be managed through containment and potentially need to undergo corrosion compatibility testing.**	**Significant sensor down-sizing is required and additional electronics may need to be down-sized and co-deployed with the sensor in the air-slots to manage signal attenuation effects from cables. An experimental multi-layer coil design for the sensor is also proposed to eliminate the need to robotically rotate the sensor inside air-slots.**	**Significant size and weight reduction would be required, which would be accompanied by a high risk of negative impact to sensor performance.**
Impact of motion requirements on the complexity of the robotic delivery system	**Two sensors are used that would require two air-slot robots to be deployed in the same and adjacent air-slots. Rotation and translation routines needed to satisfy the full suite of flaw detection capability must be done in a coordinated fashion with high spatial (0.25 in.) accuracy to support reliable signal processing and flaw detection.**	The sensor must be pressed against the tank bottom regardless of the couplant used. A dry couplant would require a higher force of 20–50 lb. No sensor rotation is required.	The sensor must be rotated inside the air-slots if the multi-layer sensor coil design is not pursued or does not work.	If the weight of the sensor system cannot be reduced to 50–100 pounds, then the robotic delivery system will need to be engineered to bear significant weight. This will be especially important for sensor support if power is lost.
Range	Demonstrated range during testing was 36–48 in., depending on the sensor configuration.	Demonstrated range during testing was 5–7 feet, limited by the test mock-up size.	**Demonstrated range in the presence of a slurry is 6–10 in.**	Demonstrated range during testing was up to 14 ft., limited by the length of the test mock-up.

3.3 Final Scoring

The final score assigned to each sensor technology at the conclusion of the evaluation process was calculated based on weighting factors applied to the raw scores for each criterion under each of the evaluation categories (flaw detection, sensor attributes, and deployment trade-offs).

The raw scores under the flaw detection category were given a weighting factor of one since the point value associated with each of the 25 flaws had been weighted prior to testing based on the level of detection difficulty.

The ten criteria for sensor attributes and the ten criteria for deployment trade-offs were weighted by a factor of one, three, or five based on the level of impact/risk to the NDE Technology Development Program and future tank inspections, as determined by WRPS. A weighting factor of one, three, and five corresponded with low, medium, and high risk/impact.

The weighting factors selected for each criterion and the justification for selection of the weighting factor are provided in Tables 8 and 9. The final scores assigned to each sensor technology after applying the weighting factors to the raw scores in Appendix H are provided in Table 10.

Table 8. Sensor Attribute Weighting Factors

Sensor Attribute	Maximum Possible Raw Score	Weighting Factor 1=Low 3=Medium 5=High	Maximum Possible Weighted Score	Justification
Surface prep requirements	5	3	15	The tank bottom is not expected to have poor surface conditions and surface preparation (e.g., scraping) would place a moderate level of burden on a robotic delivery system.
Tolerance for loose surface material	5	3	15	The tank bottom is not expected to have poor surface conditions and dirt/debris removal (e.g., brushing) would place a moderate level of burden on a robotic delivery system.
Sensor weight	5	5	25	Higher payloads would place a higher level of burden on a robotic delivery system deployed in restricted access environments.
Couplant requirements	5	5	25	Liquid couplant application and removal place a high level of burden on a robotic delivery system deployed in restricted access environments. The use of liquid couplant may also require corrosion compatibility testing.
Motion requirements	5	5	25	Elaborate sensor motion routines would place a higher level of burden on a robotic delivery system and increase the risk of measurement integrity issues.
Application and removal force	5	3	15	Higher levels of force needed to apply, remove or move a sensor would place a moderate level of burden on a robotic delivery system.
Size	5	1	5	Sensor size is important; however, all candidate sensors are or could be adapted to fit through the access riser, annulus and refractory pad air-slots.
Time to adapt sensor	5	1	5	The time for sensor adaption will influence the duration of the program; however all candidate sensors could be adapted in a 6–12 month timeframe that is considered reasonable.
Cost to adapt sensor	5	1	5	The cost for sensor adaptation is an important factor, but the cost estimates for the candidate sensors is considered reasonable.
Data quality - SNR	5	5	25	Higher SNR increases the confidence of accurate flaw reporting.
Total Points Available	50 (Raw)		**160 (Weighted)**	

Table 9. Deployment Trade-off Weighting Factors

Deployment Trade-off	Maximum Possible Raw Score	Weighting Factor 1=Low 3=Medium 5=High	Maximum Possible Weighted Score	Justification
Wall thinning	4	3	12	Wall thinning is a flaw type of concern; however, it is not higher priority than pitting or weld seam openings.
Pinwheel region defects	3	3	9	The pinwheel weld region is considered to be of moderate importance.
Blind flaws	3	5	15	The ability to detect flaws without prior knowledge of their location is of high importance.
Vulnerability to obstructed air-slots	5	5	25	Higher dependency on air-slots access (quantity and axial distance) increases the risk of inspection upset, thereby reducing overall extent of tank bottom examination.
Vulnerability to mill scale	3	5	15	There is an equal probability of mill scale being on the tank bottom as the tank sidewall, where mill scale has been encountered.
Vulnerability to pitted coupling surface	3	1	3	Not a high probability scenario given external corrosion is less probably than internal corrosion.
Adaptation risk	5	5	25	Higher risk introduces more schedule and cost uncertainty to the program timeline.
Commercial state	5	3	15	The candidate sensors are perceived to be capable of commercialization, if not already there.
Cables/in-tank electronics	5	3	15	A higher quantity of cables increases the complexity of a cable management system; in-tank electronics increases the payload and burden on a robotic delivery system.
Replacement cost of in-tank sensors/ components	5	1	5	The replacement cost of sensors, electronics and components is important; however, the costs associated with the candidate sensors is considered reasonable.
Total Points Available	41 (Raw)		**139 (Weighted)**	

Table 10. Summary of Final Weighted Scores for Flaw Detection, Sensor Attributes, and Deployment Trade-offs per Sensor

	Ultrasonic Guided Wave Sensor Option	Total Score	Flaw Detection Subtotal (of 83)	Sensor Attribute Subtotal (of 160)	Deployment Trade-off Subtotal (of 139)	Key Benefits	Key Trade-offs
Air-slot	Single-sensor piezoelectric (Guidedwave)	333	78	144	111	•Single air-slot deployment •Simple image-based analysis •High signal-to-noise ratios	•Low sensitivity to gradual wall thinning •Moderate sensor modification required •Requires 20–50 lb. force applied
	Single-sensor EMAT (Innerspec)	320	75	148	97	•Single air-slot deployment •No couplant required	•Significant sensor modification required •Analysis is more difficult (A-scan based)
	Dual-sensor EMAT (Penn State)	310	81	142	87	•Sensor size deployment ready •No couplant required	•More intensive deployment; requires two open and adjacent air-slots plus coordinated sensor rotation and translation with high spatial accuracy
Remote	Single-sensor EMAT (SwRI)	290	59	139	92	•No under-tank access required •No couplant required	•Least sensitive to in-weld defects •Not sensitive to gradual wall thinning •Significant sensor modification required to reduce size and weight

4.0 Conclusions

The objectives of Phase I of the NDE Technology Development Program were to conduct testing to determine the extents to which the candidate sensor technology options can satisfy flaw detection requirements, and to uncover gaps between examination requirements and technology performance. The objectives of Phase I were met through the FY2017 and first-quarter FY2018 testing and evaluation work summarized here.

The Phase I evaluation results revealed the following:

- There are differences in the extents to which flaw detection requirements can be satisfied by the general class of air-slot sensor technology versus the remote examination technology. As shown in Table 3, the flaw detection performance of the three air-slot sensor technology options is superior to that of the remote examination technology. All three air-slot sensor technology options performed well with each having successfully detected flaws in over 90% of the flaw scenarios. The remote examination technology detected flaws in approximately 70% of the flaw scenarios.
- There are differences in the extents to which each candidate air-slot sensor and the candidate remote examination sensor technology can satisfy flaw detection requirements in their current states. The mapping of aggregate sensor performance against the Phase I flaw matrix in Table 4 uncovered the flaw detection strengths and weaknesses of each sensor. The remote examination technology was sensitive to base plate pits plus most pits and notches in straight welds, but missed gradual wall thinning and flaws in the 90-degree weld confluence. The air-slot sensor technology options have different flaw detection strengths—the single-sensor EMAT technique (Innerspec) detected all flaw types at the actionable level value and most flaws at the reportable level values; the dual-sensor EMAT technique (Penn State) detected all flaw types at the reportable and actionable level[(a)] values; and the piezoelectric phased-array technique (Guidedwave) detected all flaw types at the reportable and actionable level values, except gradual wall thinning.
- Specific gaps exist between the abilities of today's candidate sensors and the flaw detection requirements in terms of flaw types, sizes, and the potential flaw location scenarios that were tested. The impact of these gaps is considered low and can be risk-mitigated with targeted examinations of specific tank regions (e.g., 90-degree weld confluence) using air-slot transducers, or development of supplementary remote examination NDE techniques under a separate project with a timescale that is conducive to technology development.
- Each sensor technology has leading risks that are either concentrated in the sensor maturation phase or concentrated in the sensor deployment phase. The highest leading risks for each sensor were provided in Table 7. The highest-risk attributes and trade-offs would either need to be accepted or managed through investment in research/technology development for the sensor or the robotic deployment system.

The Phase I sensor evaluation results provided here are intended to support the final programmatic goal of Phase I, which is to identify one or more sensor technologies for maturation under Phase II of the NDE Technology Development Program. A level of risk acceptance will be necessary with any sensor(s) selected for maturation under Phase II. These results should provide a well-rounded set of information to support the final sensor selection process.

(a) During *Sensor Effectiveness Testing*, Penn State did not report on the 10% wall thinning, T1, and the 50% notch located in the 90-degree weld confluence, N7, due to failure to record the data at the time of testing. After *Sensor Effectiveness Testing*, Penn State acquired additional data on T1 and N7 using the same instrumentation and settings used previously and was able to detect both T1 and N7.

The following considerations are recommended to support the decision process:

(a) Combine remote examination with air-slot examination for strategic under-tank examinations.

The Phase I test and evaluation results show that the air-slot sensor options are the best suited for providing the greatest extent of flaw detection requirement satisfaction. However, regardless of the final air-slot sensor(s) selected for maturation under Phase II, the deployment of air-slot sensors of any variety will require a basis for entering air-slots if the examinations are to be strategic instead of random or based solely on the availability of unobstructed air-slots. The selection of air-slots for sensor deployment could be risk-informed and based on higher-risk tank regions, or based on the results of preliminary screening of the tank bottom condition.

The remote examination technique detected the least number of surrogate flaws; however, its ability to detect surrogate pits in the base plate and welds and its ability to detect surrogate weld seam openings/cracks in welds (other than the 90-degree weld confluence) could provide a means for identifying potentially flawed tank bottom regions that should be examined further with air-slot sensors for higher sensitivity and resolution flaw detection. Remote examination with at least one of the three air-slot deployed NDE technologies can satisfy a proposed examination strategy that would provide an under-tank inspection approach that is more reliable and efficient than a single sensor alone. The approach would include:

a. Initially employing remote NDE technology to rapidly screen the primary tank bottom from the primary tank wall. The data would be used to identify potentially flawed tank bottom regions and the air-slots that correspond with these regions.
b. Subsequently employing NDE sensors on the primary tank bottom in air-slots beneath the potentially flawed tank regions indicated during screening to obtain higher-resolution data.

(b) Base the final selection of air-slot sensor technologies on an optimal balance between flaw detection performance and the leading risks that are acceptable.

All three air-slot sensors performed well during flaw detection testing, with each having successfully detected flaws in over 90% of the flaw scenarios. If only one air-slot sensor technology is ultimately selected for maturation under Phase II of the NDE Technology Development Program, then it is recommended that the selection be based on the highest score associated with the leading risks that WRPS finds acceptable.

5.0 References

Bandyopadhyay K, S Bush, M Kassir, B Mather, P Shewmon, M Streicher, B Thompson, Dv Rooyen and J Weeks. 1997. *Guidelines for Development of Structural Integrity Programs for DOE High-Level Waste Storage Tanks*. BNL-52527, Brookhaven National Laboratory, Upton, New York.

Boomer KD, AJ Feero and JR Gunter. 2016. *Double-shell Tank Integrity Project Plan*. RPP-7574, Rev. 4, Washington River Protection Solutions, Richland, Washington.

Follett JR. 2017. *Leak Inspection Report for Tank 241-AY-102*. RPP-RPT-60320, Rev. 0, Washington River Protection Solutions, LLC, Richland, Washington.

Moran TL, MR Larche, KM Denslow and SW Glass III. 2017a. *NDE Technology Development Program for Non-Visual Volumetric Inspection Technology – Technology Screening Report*. PNNL-26328, Rev. 0, Pacific Northwest National Laboratory, Richland, Washington.

Moran TL, MR Larche, KM Denslow and SW Glass III. 2017b. *NDE Technology Development Program for Non-Visual Volumetric Inspection Technology – Sensor Effectiveness Testing Report*. PNNL-26603, Rev. 0, Pacific Northwest National Laboratory, Richland, Washington.

Venetz TJ and JR Gunter. 2014. *Double-Shell Tank Construction: Extent of Condition*. TOC-PRES-14-1370, Rev. 0, Washington River Protection Solutions, Richland, Washington.

Appendix A – NDE Technology Development Program for Hanford DST Non-Visual Volumetric Inspection Technology: Sensor Effectiveness Testing Report From Penn State, Addendum #2

NDE Technology Development Program for Hanford DST Non-Visual Volumetric Inspection Technology: Sensor Effectiveness Testing Report From Penn State

Addendum #2

The Pennsylvania State University
University Park, PA 16802

Cliff J Lissenden, Lissenden@psu.edu
Parisa Shokouhi, parisa@engr.psu.edu

15 August 2017

We were recently contacted by Bill Glass, who indicated that we could submit additional materials to our report on sensor effectiveness testing (SET). This addendum to our report dated 21 June 2017 contains two sections:

1. Results for detection of flaw T1 on the modified mockup;
2. Results for detection of flaw N7 on the new mockup.

1. Results for detection of flaw T1 on the modified mockup

We noted in our SET report that during the mockup testing at PNNL we inspected the modified mockup for wall thinning defect T1, but we failed to record the data that was acquired. On 1 August 2017 Cliff Lissenden was at PNNL conducting an inspection of a dry storage canister mockup using the same instrumentation (except for the sensors) that was used for SET. Therefore, he had an opportunity to acquire data using the same test setup as before.

Defect coordinates and size: T1 (10,56), 4" diameter, 0.05" deep cavity

Method: Through Transmission, Transmitter T @(4-15,32), Receiver R @(4-15,72), 12 A-scans

The figure below shows the corresponding B-scan obtained by stacking the envelope of individual records. The x-axis is the x-coordinate of the mockup whereas the y-axis shows the travel distance of wave packets measured from the transmitter (T). The T1 flaw reduces the amplitude of both the SH0 and SH1 modes at x=9"-11". Note that the SH1 wave is dispersive and has a higher amplitude, making it a better indicator of the T1 flaw. The SNR is 7 dB. This value is obtained based on the amplitude reduction of SH1 mode using the expression given in our SET report. Even though the depth of T1 is only 10% of the wall thickness it is clearly detected. Moreover, the type of indication (reduction of SH1 amplitude) helps characterize the defect as wall thinning.

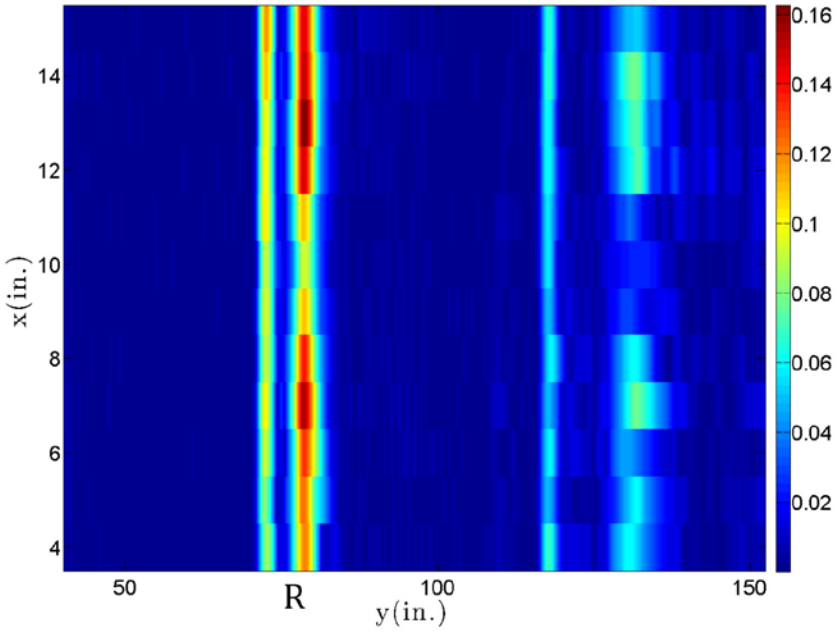

2. Results for detection of flaw N7 on the new mockup

We noted in our SET report that during the mockup testing at PNNL a bookkeeping error kept us from collecting data on notch defect N7. We inadvertently marked N7 on the 'detected flaws' checklist, and thus thought that it had been detected, when in reality it had not. On 1 August 2017 Cliff Lissenden was at PNNL conducting an inspection of a dry storage canister mockup using the same instrumentation (except for the sensors) that was used for SET. Therefore, he had an opportunity to acquire data using the same test setup as before.

Defect coordinates and size: N7 (25, 96), 2.875" long, 0.25" deep, along weld at y=96", left edge of notch is at weld at x=24"
Method: Pitch-Catch, Transmitter T fixed @(19,90), Receiver R @(37,90-75), 16 A-scans
The photograph shows the sensor positions relative to the notch and welds. Only the receiver was moved during the scan in the marked direction.

The incident wave impinges upon the weld and flaw at an average angle of 45 degrees. However, the sound beam is diverging and so the diffracted waves travel in many different directions, making analysis with SAFT very helpful for visualization. The image below was created using SAFT and shows a clear indication of notch N7 with a SNR of 15 dB.

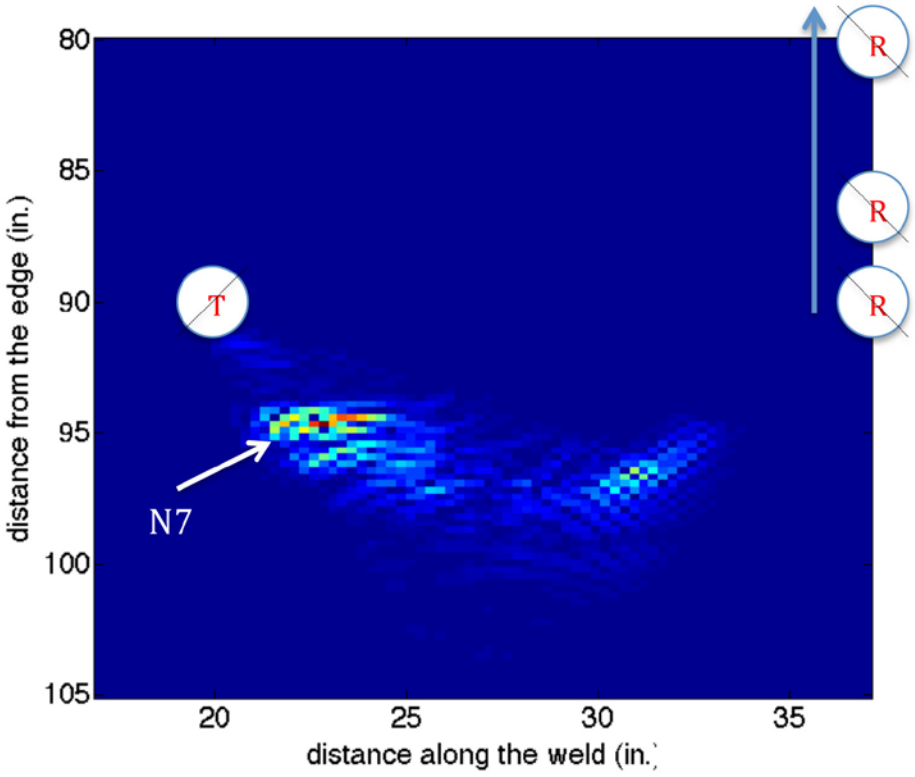

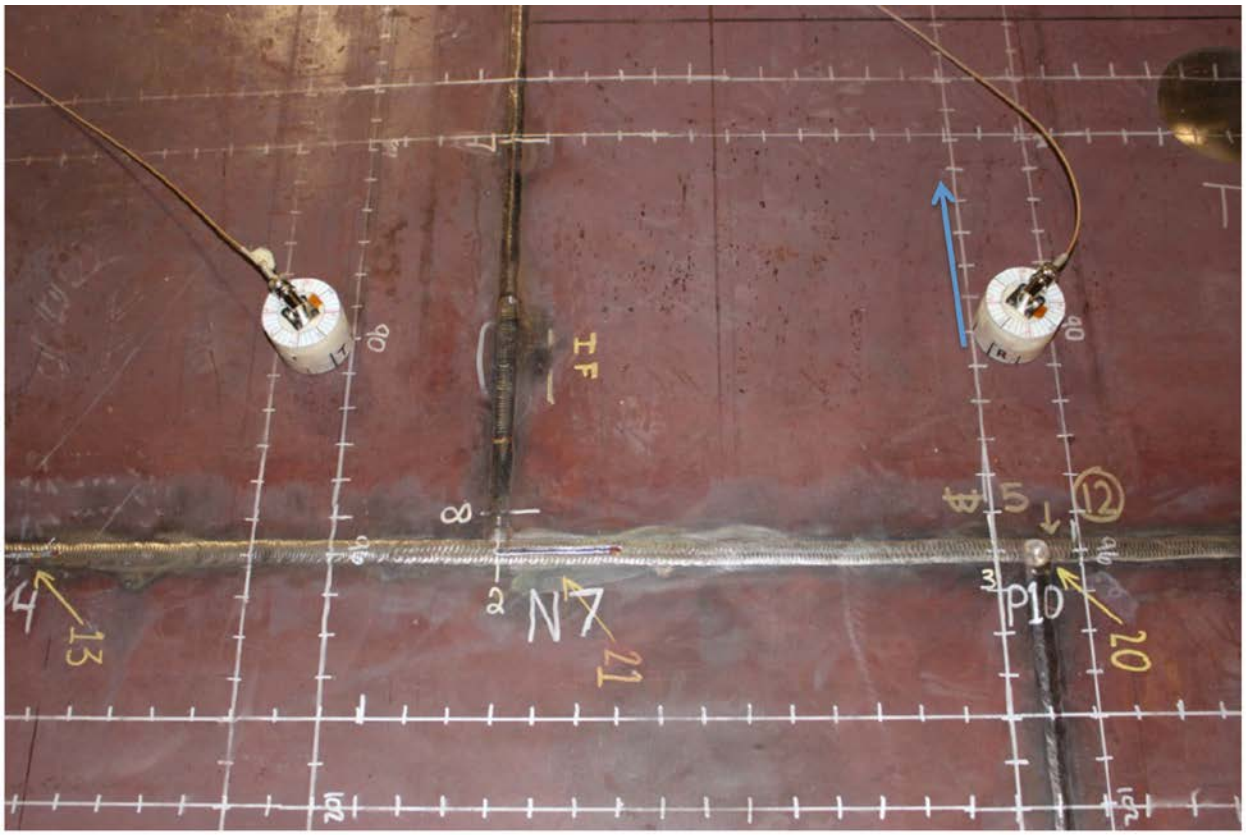
90
IF
8
2
N7
11
4
13
3
P10
20
5
12
90

Appendix B – Dry-Coupling for Guided Wave Phased Array Technology

Dry-Coupling for Guided Wave Phased Array Technology

Addendum to Hanford DST Sensor Effectiveness Testing report to demonstrate dry-coupling method for GWPA technology.

Subcontract #: 63295

performed for:

Washington River Protection Solutions, LLC
P.O. Box 850
Richland, WA 99352, USA

provided by:

Cody Borigo, cborigo@gwultrasonics.com
Russell Love, rlove@gwultrasonics.com
Steven Owens sowens@gwultrasonics.com
Guidedwave
450 Rolling Ridge Drive
Bellefonte, PA, USA 16823
+1-814-234-3437

28 July, 2017

Introduction

This document is an addendum to the Report on Guided Wave Phased Array Sensor Effectiveness Testing for Hanford DST Inspection, submitted on 28 June, 2017 to PNNL and WRPS. The purpose of this additional material is to demonstrate the capability to dry-couple the guided wave phased array (GWPA) probe, i.e. to collect GWPA data without the challenges associated with the shear couplant used with the technology during prior testing. The shear couplant was a concern for WRPS and PNNL due to the additional challenges associated with dispensing, applying, and cleaning the couplant during remote testing. The development of a proprietary dry-coupling solution will circumvent those challenges without reducing the effectiveness of the technology.

Guidedwave ◦ *The Guided Wave Innovations Company*
450 Rolling Ridge Drive ◦ Bellefonte, PA ◦ 16823
(814) 234-3437 ◦ www.gwultrasonics.com

Mockup Test Results

To characterize the performance of the new coupling methods, comparison tests were conducted on the new dry-coupled configuration and the conventional shear gel-coupled configuration that was used during testing at PNNL. The test specimen was a 48" x 48" x 0.080" aluminum panel with three manufactured flaws, as shown in Figure 2. The flaws included a 0.65" x 0.05" notch, a 0.25"-diameter through hole, and a 0.375"-diameter through hole. Data was collected with the probe in the center of the plate and 25 dB of receiver gain; this is approximately 20 dB less than was used during testing at PNNL, due to the smaller size of the test structure.

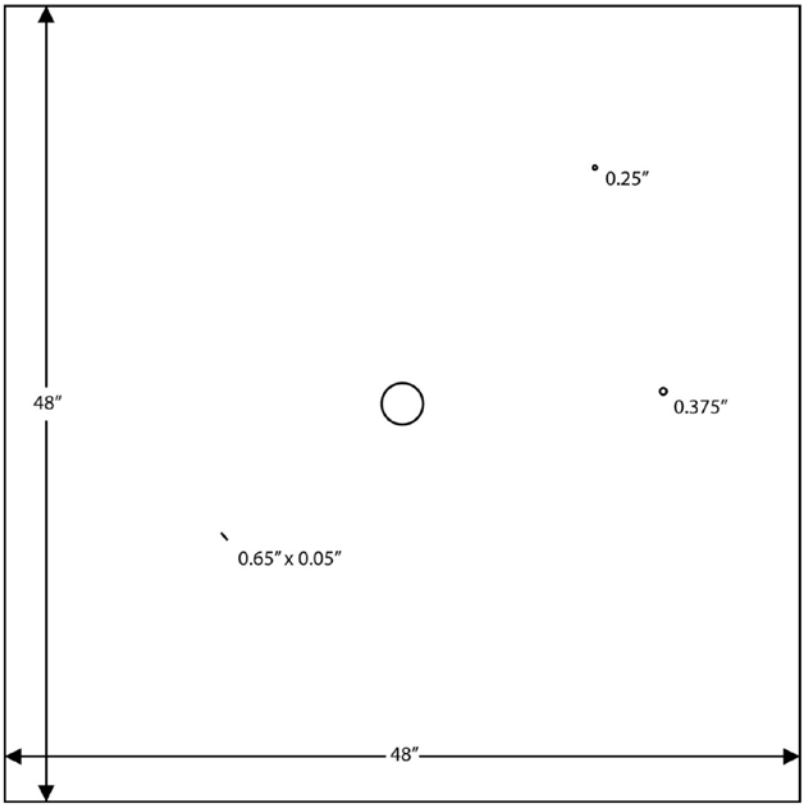

Figure 1 Drawing of the test panel used for couplant method comparison testing; the panel includes three manufactured flaws: two holes and one notch.

Figure 2 compares the GWPA images for both coupling methods ("shear gel" vs. "dry") normalized to 12 dB above the edge reflection amplitude. Not only is the signal quality comparable to the conventional gel coupling, but it is actually improved in some respects. The signal-to-noise ratio (SNR) of the notch is 47 dB for both scans and the SNR of the holes is 32.4 dB with shear gel vs. 33.7 with dry coupling. The dead zone radius is slightly larger with the dry coupling, at 5.5" vs. 5.2", but the sidelobe artifacts caused by the notch defect,

which appear as additional indications between the two hole defects and the probe, are reduced substantially. Figure 3 compares the same two scans with the C-filter applied.

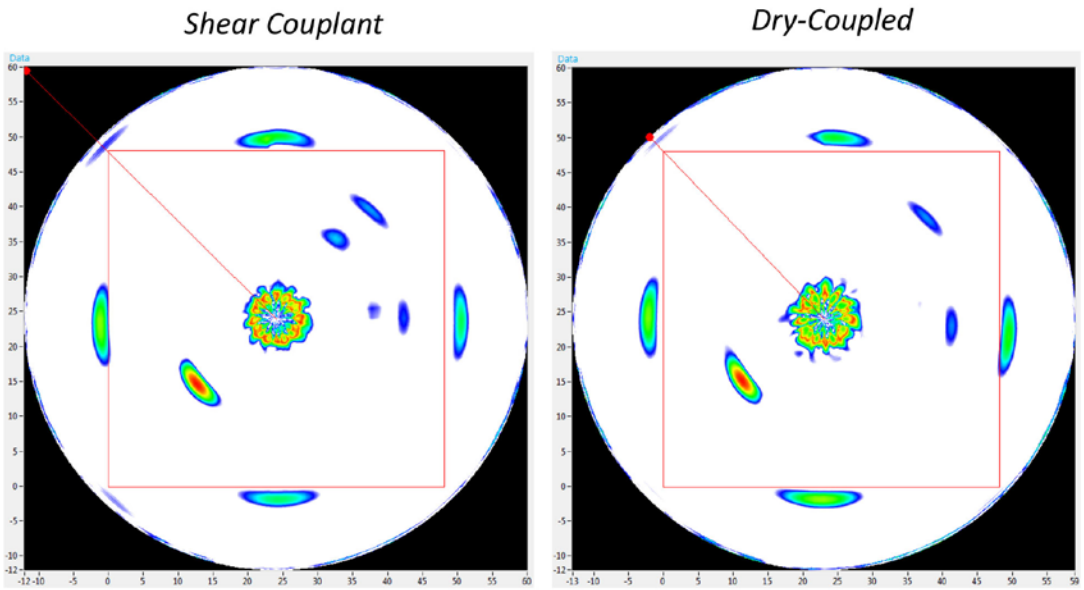

Figure 2 Comparison of the GWPA scan using the conventional shear couplant method (left) and the new dry-coupled method (right).

Guidedwave ◦ *The Guided Wave Innovations Company*
450 Rolling Ridge Drive ◦ Bellefonte, PA ◦ 16823
(814) 234-3437 ◦ www.gwultrasonics.com

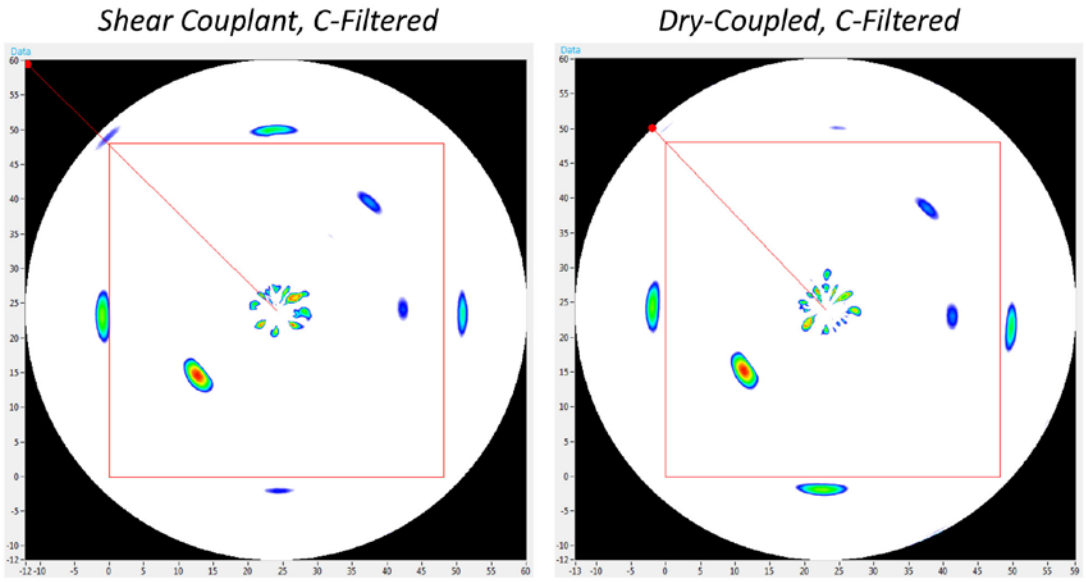

Figure 3 Comparison of the GWPA scan using the conventional shear couplant method (left) and the new dry-coupled method (right).

Guidedwave is going to conduct further testing to optimize the dry coupling solution, comparison test on various surfaces, and designing an easy-to-apply prepared dry-coupling membrane system for even easier field use.

Force Requirements

Tests were conducted with the dry-coupling mechanism using varying static loads applied to the back of the probe. Loads of from 5 to 50 lbs were applied 5 lb increments, and the signal attributes were compared to each other and those of a probe coupled directly with shear gel couplant. Figure 4 compares the plate edge and notch defect SNR for the two coupling mechanisms versus load. For this measurement, a higher value is better. The shear gel-coupled probe SNR was generally independent of applied load, while the dry-coupled probe SNR increased with load, but leveled off near the values for the gel-coupled probe near 40 lbs.

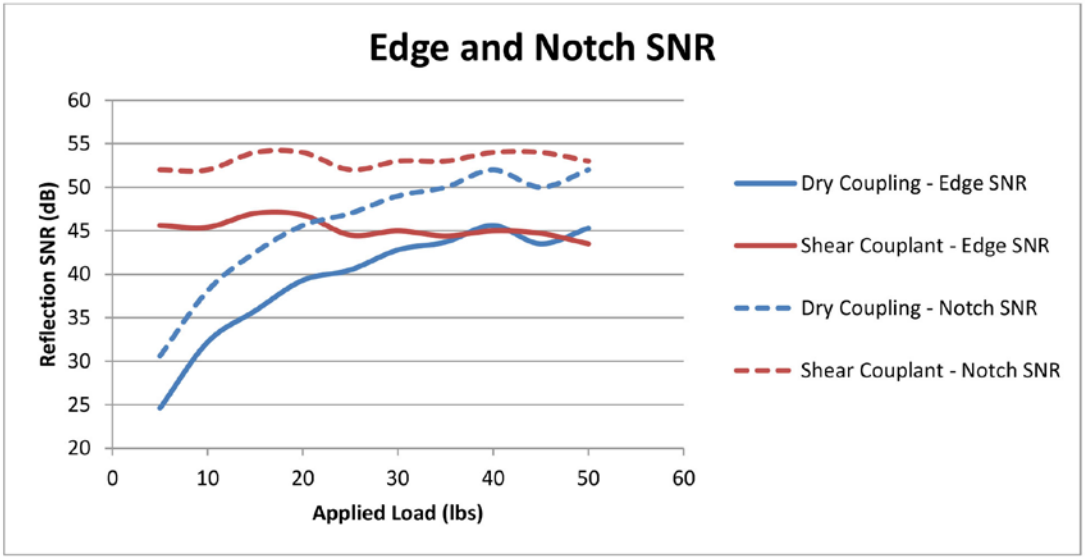

Figure 4 Edge and notch SNR values (in dB) for both coupling mechanisms versus load.

Figure 5 compares the maximum raw signal amplitude from the notch reflection (in mV), measured prior to phased array post-processing, for the two coupling mechanisms versus load. For this measurement, a higher value is better. The shear gel-coupled probe signal amplitude gradually decreased with load, but started at a high level, while the dry-coupled probe signal amplitude increased monotonically with load.

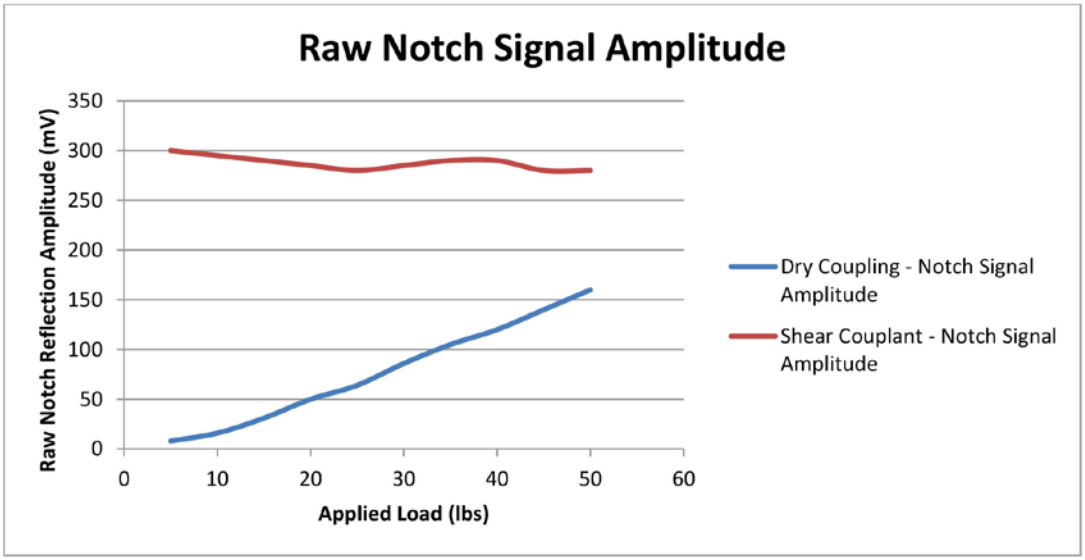

Figure 5 Max raw signal amplitude from the notch reflection for both coupling mechanisms versus load.

Figure 6 compares the sidelobe amplitude from the notch reflection for the two coupling mechanisms versus load. For this measurement, a lower value is better. The shear gel-coupled probe sidelobes were stronger and got worse with load, while the dry-coupled probe sidelobes were weaker and generally improved with load.

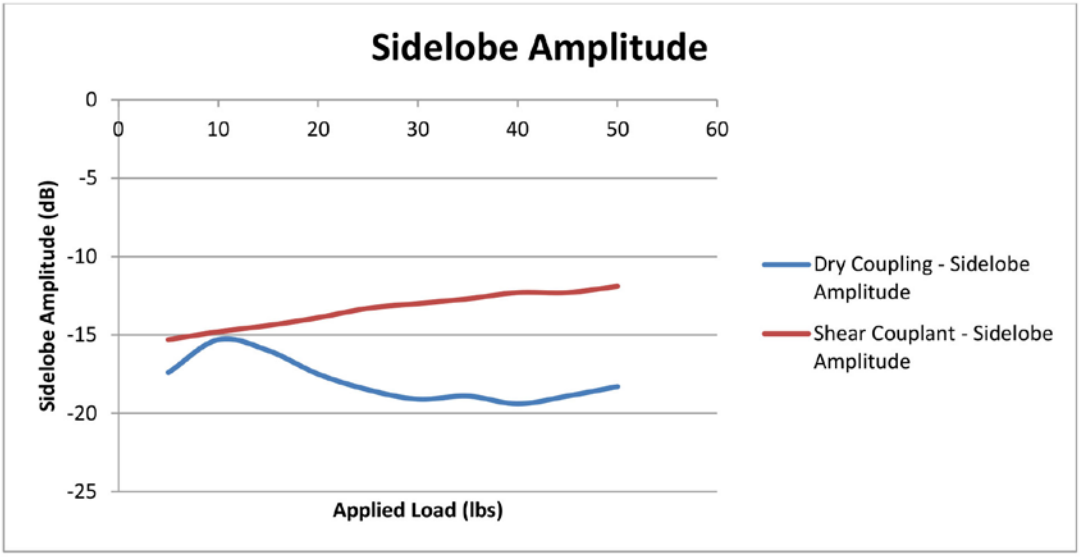

Figure 6 Sidelobe amplitude for both coupling conditions versus load.

Figure 7 compares the dead zone radius for the two coupling mechanisms versus load. For this measurement, a lower value is better. The shear gel-coupled probe dead zone was small and constant with load, while the dry-coupled probe dead zone was larger and rapidly decreased with load, approaching the value for the gel-coupled probe around 50 lbs.

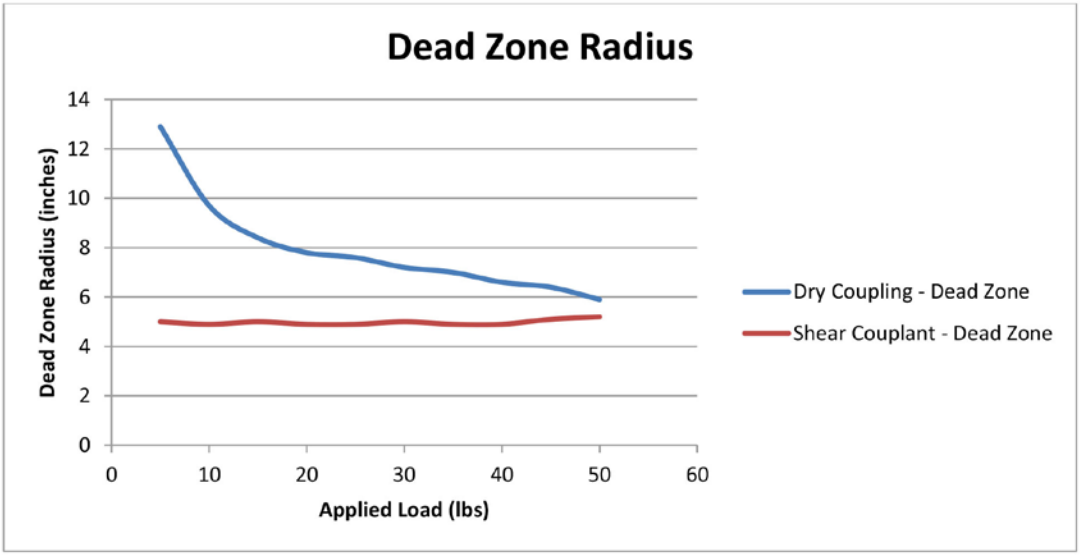

Figure 7 Dead zone radius for both coupling mechanisms versus load.

Shear Couplant Corrosion Effects

While we are still waiting to receive a response from the manufacturer of a commercially-available shear gel couplant regarding corrosion-causing compounds, we did find some general information that appears to demonstrate that there should be no corrosion concerns from the couplant, if any were to be left in contact with the surface. The manufacturer's data sheet claims that the shear gel couplant features "very good corrosion inhibition". Further study revealed a general consensus that honey is actually an excellent corrosion inhibitor for many metals; remember that the shear gel couplant is simply processed honey. For instance, see A.Y. El-Etre and M. Abdallah, "Natural honey as corrosion inhibitor for metals and alloys. II. C-steel in high saline water", Corrosion Science, 42(4), 2000, pp. 731-738.

Summary

The new dry coupling method for the GWPA technology further improves an already excellent NDT technique and eliminates the need for remote couplant dispensing, application, or cleanup during remote testing on the Hanford DST primary liner floors. The couplant and foil sheet can be easily applied on the surface prior to probe deployment, and the probe can be used repeatedly without reapplying any couplant by simply pressing the probe against the test surface with minimal force. There is no cleanup involved, and if the coupling membrane needs to be reapplied after a series of tests, it is a relatively simple process. The performance of the probe with the dry coupling versus gel coupling generally improves with applied load, nearing the values for the gel-coupled probe at 40-50 lbs of force for the key signal characteristics. This is a major improvement in the GWPA technology and allows it to be remotely deployed for primary liner floor inspection with great ease.

Appendix C – EMAT SV Wave for the Inspection of DSW Tank Bottoms

EMAT SV Wave for the Inspection of DSW Tank Bottoms

Demonstration for Energy Leakage in Liquid Loaded Structures at ASNT 2017

1. Executive Summary

A steel plate of 0.5" thickness of 48" length and 24" width was selected. The defects were machined on the bottom side of the sample and no information about the location of defects and their quantity was provided. The access on the plate was restricted in designated channel drawn on the sample. The objective of the test was to identify the defects while remaining in the access channels. Once defects are identified, the location of the defects must be marked and responses captured. Later the bottom of the same plate was submerged in thick slurry type liquid and responses from the same defects needs to be recorded again keeping same settings to determine the amount of possible attenuation due to the energy leaking into the liquid interface.

All tests were carried out using same type of sensor, emat coil and equipment comprising of Power Box-H (One Channel Emat Instrument) and Power BOX-MP (DC Magnet Pulser), generating SV waves 2250 kHz frequency. All the responses during this demonstration were captured using 9dB gain.

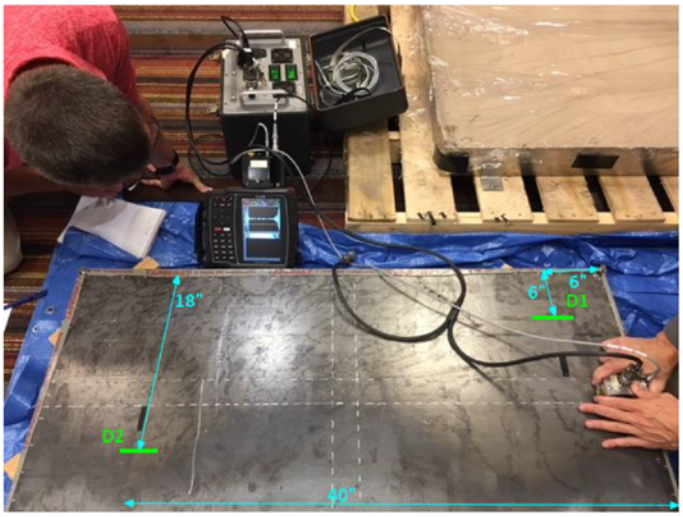

Figure-1 Sample on Floor along with Test Equipment and Sensor

We detected two defects (D1 and D2) which we think are machined notches at the location annotated in Figure-1. Looking at the amplitude of the two responses we think defect D1 is deeper as compare to defect D2. However, it is still difficult to quantify the depth of the notches due to several variables which can affect the amplitude from the defects.

2. Results

2.1. Summary

Defects	Condition	Amplitude (%)	Amplitude (dBs)	Attenuation (dBs)
D1	DRY	66%	22.4 dBs	
D2	DRY	36%	17.14 dBs	
D1	WET	23%	13.25 dBs	-9.15 dBs
D2	WET	18%	11.13 dBs	-6.02 dBs

2.2. Condition Dry – Defect D1

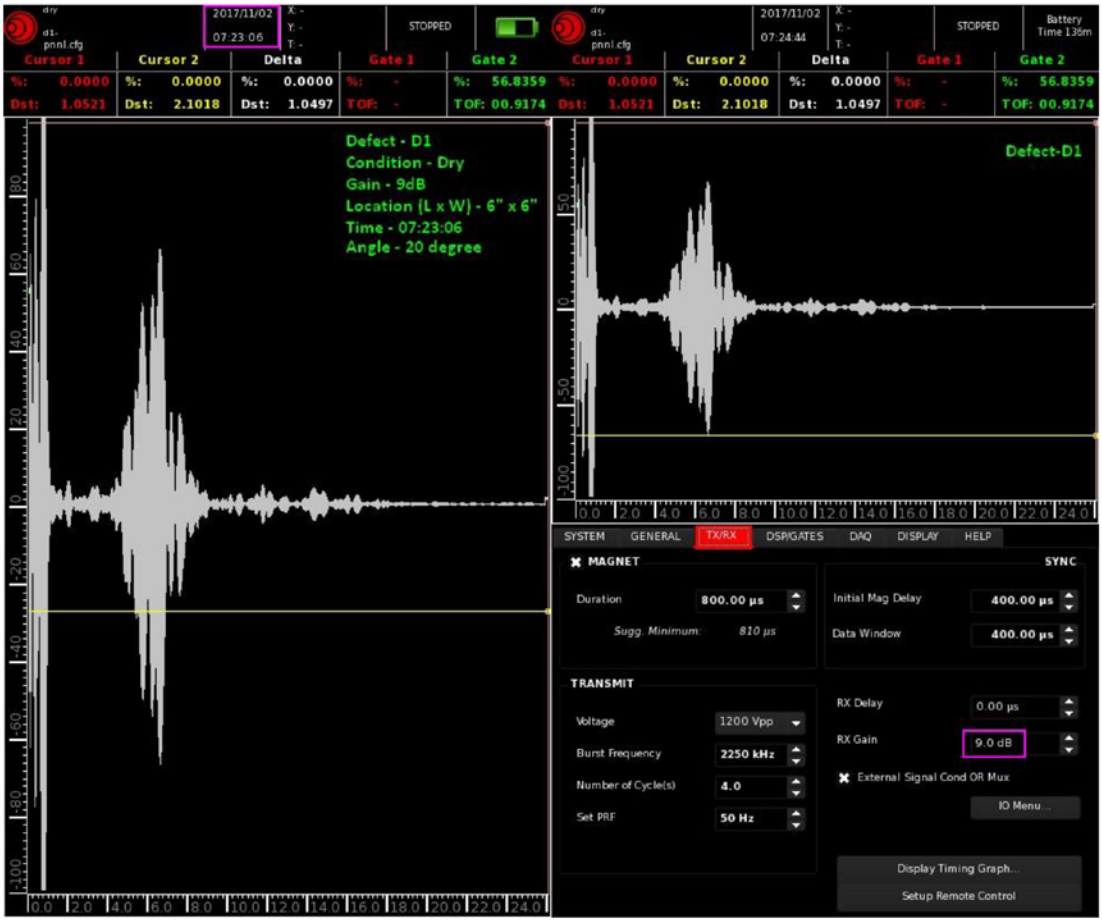

Remarks

- Amplitude of D1 – **66% (22.4 dBs)**

2.3. Condition Dry – Defect D2

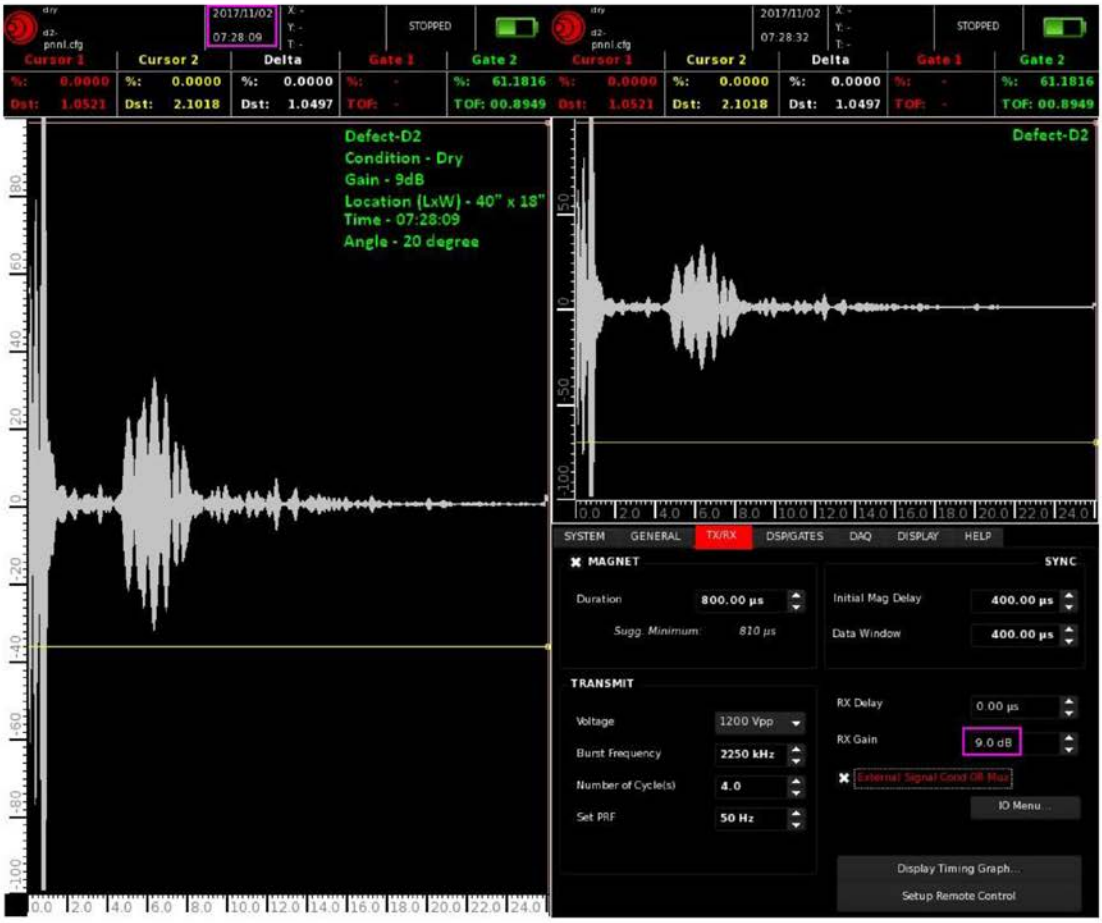

Remarks

- Amplitude of D2 – **36% (17.14 dBs)**

2.4. Condition Wet – Defect D1

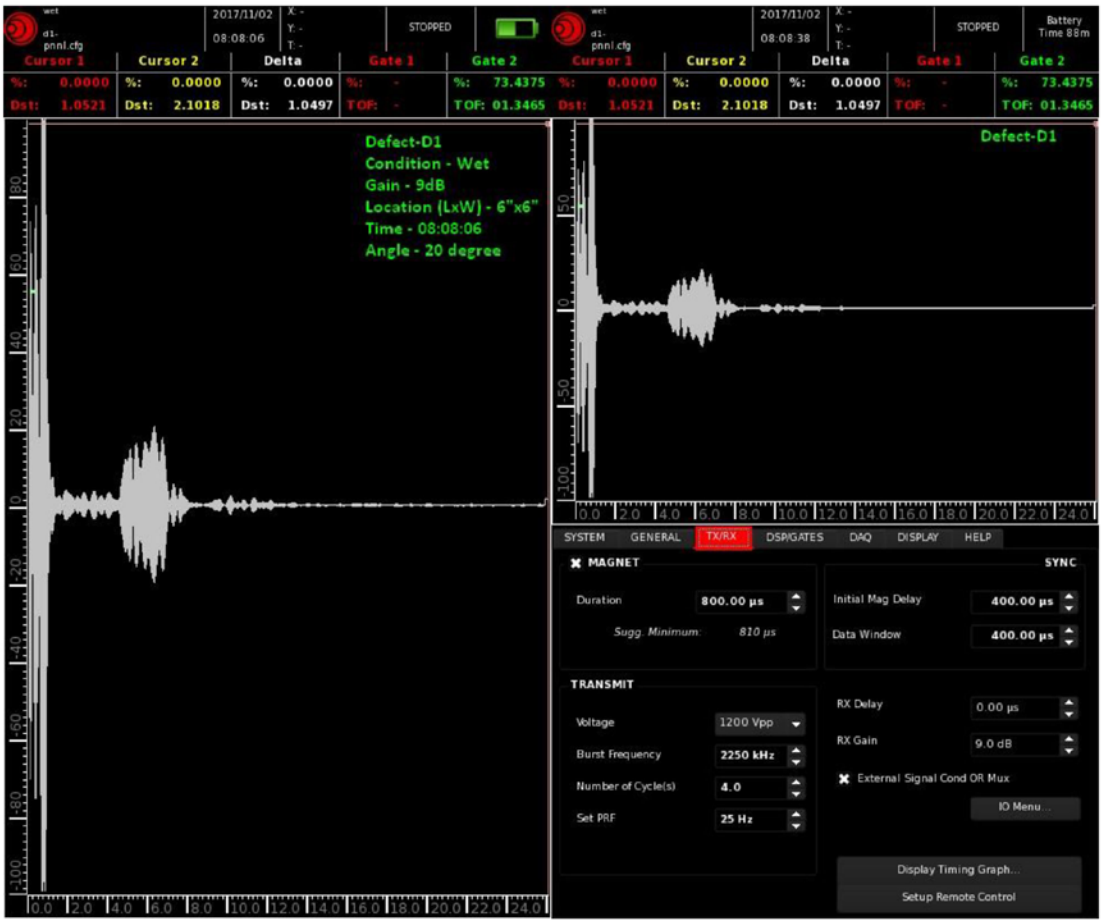

Remarks

- Amplitude of D1 – **23% (13.25 dBs)**
- Attenuation due to Energy Leakage into the liquid – (22.4 dBs – 13.25 dBs = 9.15 dBs)
  - $20log\frac{23}{66} = \mathbf{-9.15\ dBs}$

2.5. Condition Wet – Defect D2

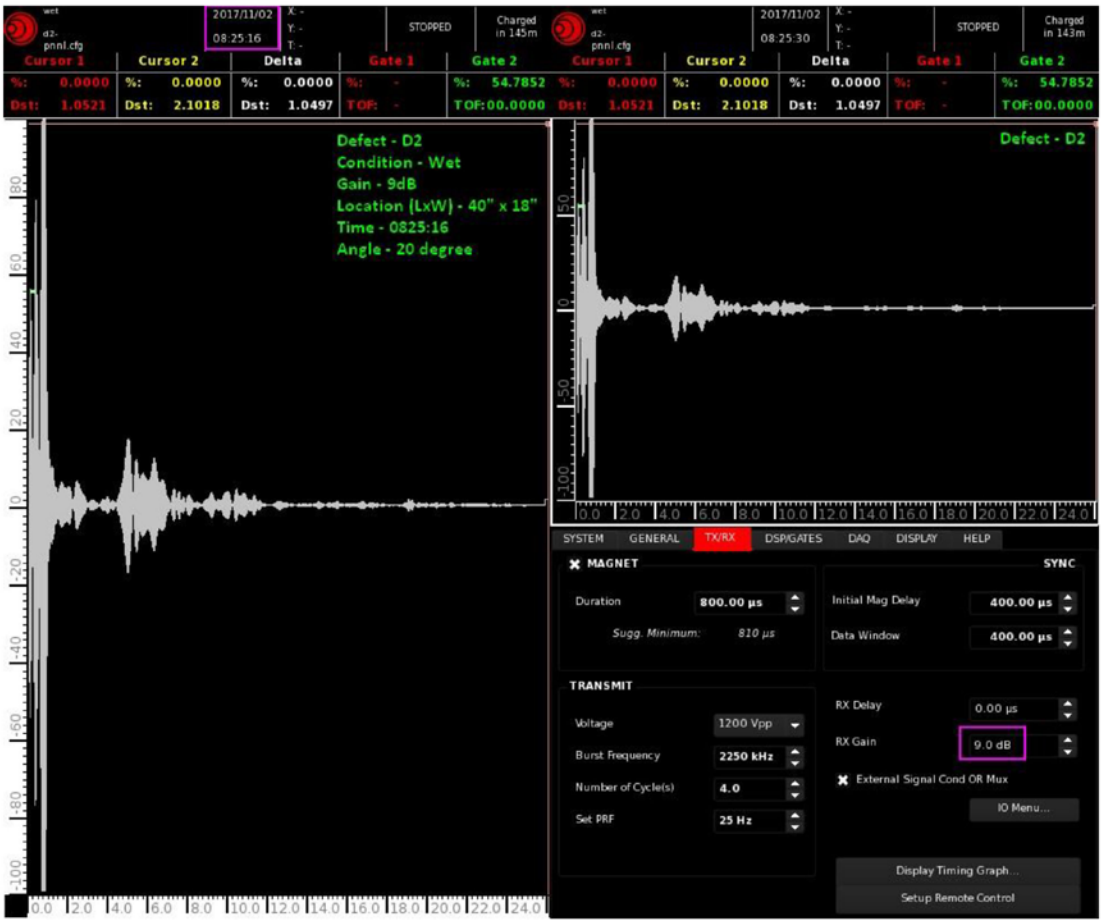

Remarks

- Amplitude of D2 – **18% (11.13 dBs)**
- Attenuation due to Energy Leakage into the liquid – (17.14 dBs – 11.13 dBs = 6.01 dBs)
  - $20log\frac{18}{36} = \mathbf{-6.02\ dBs}$

2.6. Tabulated Data

Innerspec Air-backed Plate Flaw Detection Demo					
Sensor Location on Plate	**Suspected Flaw Location**	**Time File was Saved**	**Waveform Data Filename**	**Pulser Gain Setting**	**Receiver Gain Setting**
5.5" Mid – 20° degree	6" x 6"	07:23:06 07:24:44	drydry_d1__2017-11-02_07.23.07_7.png drydry_d1__2017-11-02_07.24.45_9.png	1200V	9 dB
41.5" Mid – 20° degree	40" x 18"	07:28:09 07:28:32	drydry_d2__2017-11-02_07.28.10_12.png drydry_d2__2017-11-02_07.28.33_15.png	1200V	9 dB
5.5" Mid – 20° degree	6" x 6"	08:08:06 08:08:38	wetwet_d1__2017-11-02_08.08.06_16.png wetwet_d1__2017-11-02_08.08.38_18.png	1200V	9 dB
41.5" Mid – 20° degree	40" x 18"	08:25:16 08:25:30	wetwet_d2__2017-11-02_08.25.17_22.png wetwet_d2__2017-11-02_08.28.00_24.png	1200V	9 dB

3. Conclusion

As expected, EMAT-generated SV waves did show leakage into the liquid and attenuated the responses. It is also important to note that the mud also removed a lot of the ringing and cleaned the signals (most likely by removing some frequencies from the signal).

Other conclusions from the test:

- Due to cleaner signals, overall signal to noise was similar for both inspections.
- Assuming maximum attenuation of -9dB attenuation over 6", the instrument used still has enough gain (40dB) to provide similar signal strength for approx. 2 feet. If we used unidirectional transmitters (as expected for the final system) we could double that distance with the same signal to noise. The proposed instrument will also use our new pulser/receiver design that increases signal to noise and increases dynamic range by approximately 20dB.
- The variations in attenuation between both readings can probably be attributed to the fact that all the measurements were taken by hand with the sensor at an angle to avoid the strong reflections from the edges of the plate. The angle and sensor location on the channel will undoubtedly affect the strength of the return signals. Moreover, the size of the defects could affect the response to some frequencies that were eliminated during the tests in the mud. In this regard, it is highly recommended that before the on-site inspection the equipment is calibrated on samples with mud to simulate as best as possible the expected condition of the tanks.
- The defects were not detected when addressed from the channels going across the samples (perpendicular to the long channel). Part of the reason is that the defects were closer to the longitudinal channel, but it is also very likely that the orientation of the defects reflected more energy when addressed from the longitudinal channel (defect orientation was parallel to this channel). If distance is the issue, this could be partially compensated by using sensors with wider aperture and applying a DAC curve (the new instrument incorporates TCG).

Overall the main conclusion is that the technique still seems well suited for the application. Using our newer instrument and sensors, and proper calibration, we should significantly improve upon these results.

Appendix D – GWPA Dry Coupling Tests at ASNT Conference

GWPA Dry Coupling Tests at ASNT Conference

Test Date: 2 November 2017

Cody Borigo, cborigo@gwultrasonics.com
Guidedwave
450 Rolling Ridge Drive
Bellefonte, PA, USA 16823
+1-814-234-3437

16 November 2017

Introduction

This document summarizes the GWPA dry coupling tests conducted with PNNL and WRPS personnel at the Inn at Opryland during the 2017 ASNT Annual Conference in Nashville, TN on 2 November 2017. The primary purpose of these tests was to evaluate the performance of the GWPA system using the newly-developed proprietary dry-coupling method compared to the conventional shear gel-coupling method. A secondary motivation was to evaluate the effect of a slurry analog on the GWPA signal. Due to the very small size of the test specimen, it is not reasonable to consider this a test of flaw sensitivity.

Test Structure

The test structure was a 24" x 48" x 0.5" steel plate with a small amount of T-tape damping material on the edges. The plate was laid atop a slurry analog for some of the tests. See Figure 1. The slurry had a high viscosity that could lead to some signal attenuation of guided and non-guided ultrasonic waves, including SH waves. Based on the results of the tests, the attenuation of the SH waves was minimal over these distances.

Figure 1 Photograph of the test plate in the slurry with the GWPA system on the left.

Guidedwave ◦ *The Guided Wave Innovations Company*
450 Rolling Ridge Drive ◦ Bellefonte, PA ◦ 16823
(814) 234-3437 ◦ www.gwultrasonics.com

Test Procedure

For the shear gel-coupled tests, the shear couplant was applied in a manner similar to that used during prior testing in Richland, WA. For the dry-coupled tests, a prepared membrane was applied to the face of the transducer. A 50-lb calibration weight was placed on top of the probe during scanning, as shown in Figure 2. After the weight is removed, the probe can be easily picked up and placed in the next test position.

Figure 2 Photograph of the GWPA probe under the dry-coupling configuration with the coupling membrane and the 50-lb calibration weight present.

Limitations Due to the Test Structure

The small dimensions of the plate severely limited the ability of the technology to inspect for flaws for three reasons:

1. The noise level increased dramatically in all directions beyond the radius at which the nearest edge is encountered, as illustrated in Figure 3.
2. Due to the edge-related noise, the artifact suppression filter could not be used.
3. The artifacts caused by the edges were too numerous to be eliminated by the composite imaging process.

Each of these three negative effects are very detrimental to the imaging process, because the artifact suppression and composite imaging tools are important for generating high-quality scans. Of course, the general noise floor is also critically important for achieving maximum

sensitivity. None of these issues would be encountered during inspection of a real tank structure. Even if the plate size remained the same, but the free edges were replaced by butt welds connected to other plates, these negative effects would be drastically reduced.

As is illustrated in Figure 3, there is only a very small region (highlighted in green) of low noise outside of the dead zone and nearfield but before the noise caused by the edges.

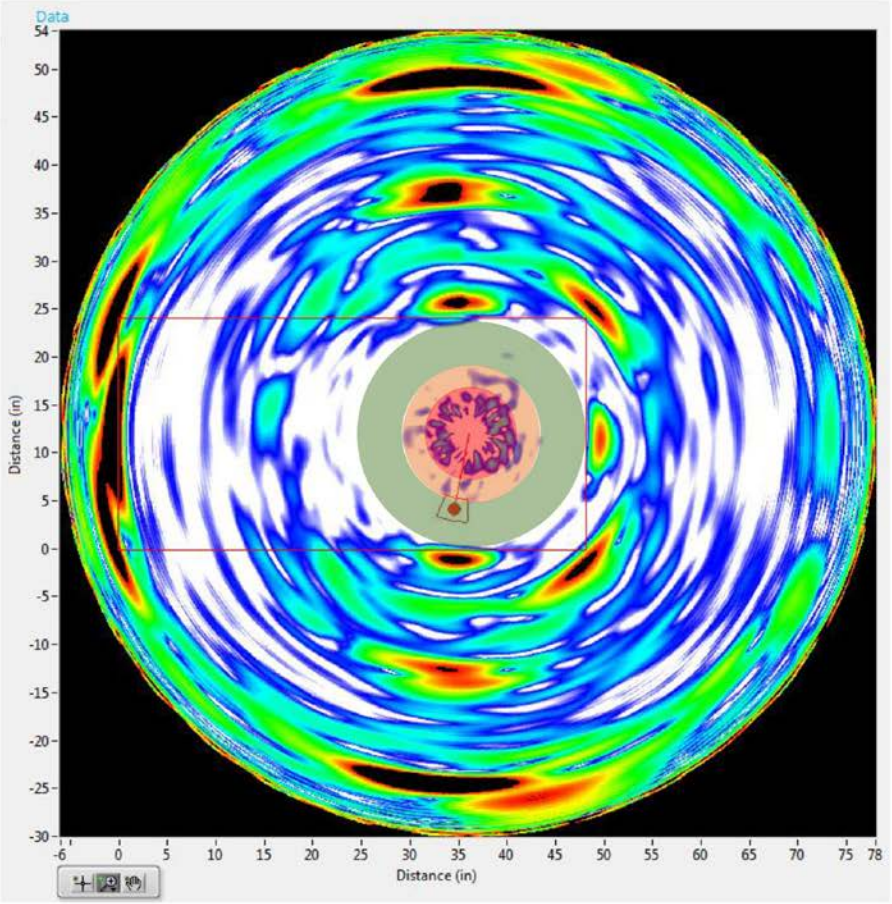

Figure 3 Example of additional noise caused by the plate edges; red area is dead zone, orange area is nearfield, and green area is low-noise region before the first edge.

Test Results

Data was collected with and without the slurry and with both dry and gel coupling. The data collected with the dry coupling on the slurry-backed plate was deemed to be invalid due to damage to the probe during shipping. Reapplying a new coupling membrane fixed the problem, but the slurry had already been cleaned from the plate. Fortunately, the effects of the coupling method and the slurry can be isolated based on the various test configurations that were considered.

GWPA data was collected on the plate in four configurations:

1. Dry-coupled, with slurry – invalid data due to damaged coupling membrane
2. Gel-coupled, with slurry
3. Dry-coupled, without slurry (bare)
4. Gel-coupled, without slurry (bare)

To evaluate the signal-to-noise ratio (SNR) under the various test conditions, the average amplitude of the four edge reflections was compared to the noise level. The noise level was determined based on the noise area outside of the scan dead zone, but before the nearest edge (the green region in Figure 3). Due to the small dimensions of the plate and the free plate edges, the "noise" level increases dramatically for the full 360° scan for all radial distances beyond the nearest edge. Due to this complication, the SNR calculations were carried out on the data from the three locations that were farthest from the plate edges: (18", 12"), (24", 12"), and (30",12"). The results are summarized in Table 1 and detailed in Table 2.

The effects of the coupling and the slurry can be independently analyzed, since they should truly be independent variables, by comparing the slurry vs. bare conditions using the gel-coupled data and by comparing the dry-coupling vs. gel-coupling methods using the bare plate (no slurry) condition. Based on this analysis, Table 1 demonstrates that the decrease in SNR for the gel-coupled tests caused by the addition of the slurry approximately 1.2 dB. Therefore, the effect of the slurry was quite small on the overall SNR achieved during these tests. Furthermore, the difference in SNR between the dry-coupled and gel-coupled data was only 0.2 dB (in favor of dry coupling), which is well within the margin of error for the SNR measurements. This is in agreement with prior internal testing performed by Guidedwave and shared with PNNL in separate reports.

Table 1 Summary of the SNR results that highlight the effects of the slurry and the coupling methods independently.

Dry-coupled vs. Gel-coupled (no slurry)	+0.2	dB
Slurry vs. No Slurry (gel-coupled)	-1.2	dB

Table 2 SNR values for plate edge reflections under various test conditions

Location 1 (24", 12")						
	Top Edge	Right Edge	Bottom Edge	Left Edge	Noise	AVG SNR
Gel - Slurry	2.8	0	5	0	42.3	**40.4**
Dry - Bare	4.6	0	4.6	0	47.7	**45.4**
Gel - Bare	5	0	5	0	46.3	**43.8**

Location 2 (30", 12")						
	Top Edge	Right Edge	Bottom Edge	Left Edge	Noise	AVG SNR
Gel - Slurry	7.8	3.6	7.1	0	42.7	**38.1**
Dry - Bare	6.4	5.7	7.5	0	48.8	**43.9**
Gel - Bare	7.8	3.9	7.8	0	46.6	**41.7**

Location 5 (18", 12")						
	Top Edge	Right Edge	Bottom Edge	Left Edge	Noise	AVG SNR
Gel - Slurry	7.1	0	7.1	4.6	56.2	**51.5**
Dry - Bare	4.8	0	5.5	2.7	48	**44.8**
Gel - Bare	8.5	0	8.5	5	53.4	**47.9**

Average of Three Locations						
	Top Edge	Right Edge	Bottom Edge	Left Edge	Noise	AVG SNR
Gel - Slurry	5.9	1.2	6.4	1.5	47.1	**43.3**
Dry - Bare	5.3	1.9	5.9	0.9	48.2	**44.7**
Gel - Bare	7.1	1.3	7.1	1.7	48.8	**44.5**

A comparison of two GWPA scans from the same position (24", 12") on the plate without slurry using the dry-coupled and gel-coupled methods is provided in Figure 4. The color scales are set to equivalent amplitudes in both plots. The reflection at ~(6",6") is most likely a flaw, and the other reflection at ~(42",18") may also be a flaw.

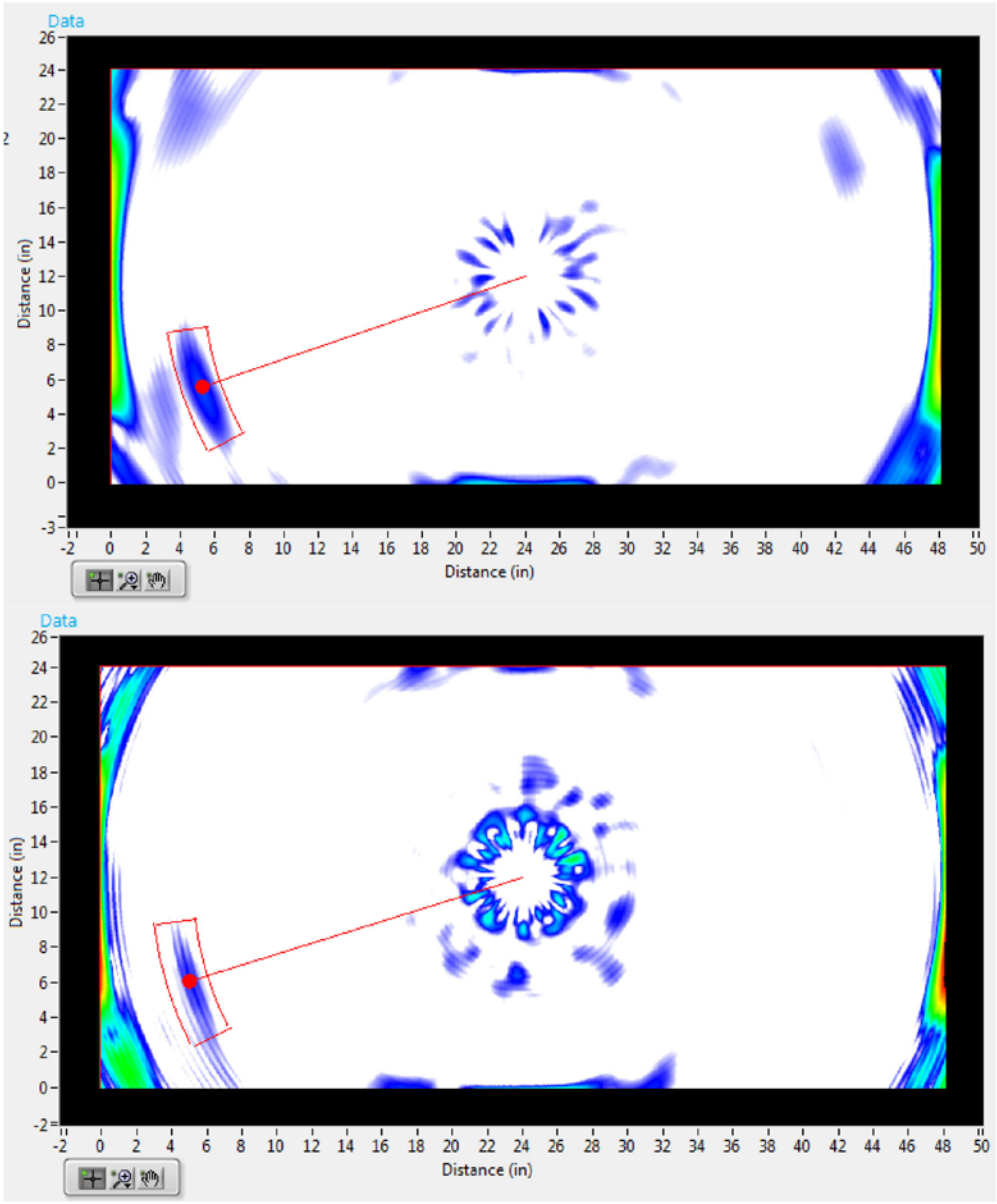

Figure 4 Comparison of the dry-coupled scan (top) vs. the gel-coupled scan (bottom) from the center position on the bare plate (no slurry), with the color scales set to comparable levels.

Summary

Due to the dimensional limitations of the plate, it was quite difficult to accurately inspect for flaws. The direct effect of the small plate size is a dramatic increase in noise in all directions after the nearest edge reflection occurs, and secondary effects stemming from this include an inability to use the powerful artifact suppression and composite imaging algorithms effectively. One flaw is clearly identified despite these limitations at approximately (6", 6"), and a second flaw may be present at approximately (42", 18"), as shown in Figure 4. However, it is worth reiterating that this is not a fair test specimen to evaluate the flaw detection sensitivity of the technique. These tests should only be viewed as an evaluation of the dry-coupled SNR versus the gel-coupled SNR and the attenuation induced by the slurry.

The effect of the slurry appears to be relatively small, as was anticipated. The test results do show that the dry-coupling method produces at least equivalent results to the gel-coupled method when a 50-lb force is applied to the dry-coupled probe. These results agree with the internal testing carried out by Guidedwave on aluminum plates and steel plates with varying degrees of surface corrosion. Further improvements to the dry coupling method could be realized through additional development efforts aimed at optimizing the membrane, as well as engineering practical systems and methods for prepping and applying the coupling membranes. Since Guidedwave has provided PNNL with three separate series of test results on the dry coupling method beyond the scope and funding of the most recent contract, any additional testing and analysis would need to be carried out under a new contract. Guidedwave would be happy to provide PNNL with a quote to perform further development and testing of the dry coupling method and any other aspects of the GWPA technology with respect to the Hanford DST primary liner inspection application.

Appendix E – Flaw Detection Performance Evaluation Criteria and Scoring System

Machined Surrogate Flaw	Flaw Depth[a]	Length and Width	Flaw ID	Flaw Location and Orientation in Mock-up	Point Value (Weighted)
Pit	25% t, 0.125 in.	0.375 in. diameter	P1	Base plate (ID)	3
Pit	25% t, 0.125 in.	0.375 in. diameter	P2	1/2-to-1/2 in. weld (ID)	5
Pit	50% t, 0.25 in.	0.75 in. diameter	P3	1/2-to-1/2 in. weld (ID), within 30° angled weld	4
Notch	20% t, 0.10 in.	2 in. long, 0.125 in. wide	N1	1/2-to-1/2 in. weld (ID), axial orientation, parallel with weld	4
Notch	50% t, 0.25 in.	2 in. long, 0.125 in wide	N2(i)	Base plate perpendicular to 1/2-to-1/2 in. weld (ID) (previously Flaw i from *Technology Screening*)	3
Notch	50% t, 0.25 in.	2 in. long, 0125 in wide	N3(m)	Base plate parallel to 1/2-to-1/2 in. weld (ID) (previously Flaw m from *Technology Screening*)	3
Wall thinning	10% t, 0.05 in.	4 in. diameter	T1	Base plate (ID)	3
Pit	50% t, 0.25 in.	0.75 in. diameter	P4	Base plate (ID)	2
Pit	75% t, 0.375 in.	1.125 in. diameter	P5	Base plate (ID)	1
Pit	50% t, 0.25 in.	0.75 in. diameter	P6	7/8-to-1/2 in. transition weld (ID)	4
Pit	75% t, 0.375 in.	1.125 in. diameter	P7	7/8-to-1/2 in. transition weld (ID)	3
Pit	50% t, 0.25 in.	0.75 in. diameter	P8	1/2-to-1/2 in. weld (ID)	4
Pit	75% t, 0.375 in.	1.125 in. diameter	P9	1/2-to-1/2 in. weld (ID)	3
Pit	50% t, 0.25 in.	0.75 in. diameter	P10	1/2-to-1/2 in. weld (ID), corner of 90° weld confluence	4
Pit	25% t, 0.125 in.	0.375 in. diameter	P11	7/8-to-1/2 in. transition weld (ID)	5
Pit	50% t, 0.25 in.	0.75 in. diameter	P12	Base plate, located beyond a 1/2-to-1/2 in. weld (ID)	3
Notch	50% t, 0.25 in.	2 in. long, 0.125 in. wide	N4	1/2-to-1/2 in. weld (ID), circumferential orientation, parallel with weld	4
Notch	50% t, 0.25 in.	2 in. long, 0.125 in wide	N5	7/8-to-1/2 in. transition weld (ID), axial orientation, perpendicular to weld	4
Notch	50% t, 0.25 in.	2 in. long, 0.125 in wide	N6	1/2-to-1/2 in. weld (ID), axial orientation, perpendicular to weld	4
Notch	50% t, 0.25 in.	2.875 in. long, 0.125 in wide	N7	1/2-to-1/2 in. weld (ID), extending from corner of 90° weld confluence, circumferential orientation, parallel with weld	5
Wall thinning	20% t, 0.10 in.	4 in. diameter	T2	Base plate (ID)	2
Wall thinning	50% t, 0.25 in.	4 in. diameter	T3	Base plate (ID)	2
Wall thinning	50% t, 0.25 in.	4 in. diameter	T4	Base plate (ID), located beyond a 1/2-to-1/2 in. weld (ID)	2
Pit	50% t, 0.25 in.	0.75 in. diameter	B1	Base plate (OD)	2
Notch	50% t, 0.25 in.	3.0 in. long, 0.125 in wide	B2	1/2-to-1/2 in. weld (OD), circumferential orientation, perpendicular to weld	4

Appendix F – Sensor Attribute Evaluation Criteria and Scoring System

Sensor Attribute Category	Criteria and Point Values (not Weighted)				
Surface prep requirements	No surface prep required. Examination conducted on as-is surface.	Minimal surface prep required (removal of dust/ dirt). Can be done with passive system (i.e., brush).	Surface prep required. Performed using active system.	Pristine surface required. Done using separate deployment with surface cleaning equipment. Removal of dirt and rust required.	Surface requires sanding/ buffing
	5	4	3	2	1
Tolerance for loose surface material	Signal unaffected by dirt/rust layer	Signal reduced by 50% or less	Signal reduced by more than 50% but still see a signal	No signal detected	
	5	4	3	2	1
Sensor weight	<10 lb.	10–25 lb.	25–50 lb.	>50 lb.	
	5	4	3	2	
Couplant requirements	No couplant required	Couplant applied/ removed during examination (applied and wiped off while scanning using passive system)	Couplant applied/ removed during examination using active system (brush/scrubber or separate mechanical system)	Separate deployment/tooling is required to apply/remove couplant	Couplant permanently attached to inspection surface
	5	4	3	2	1
Motion requirements	No additional degree of freedom is needed	Sensor requires rotation in air-slot	Coordinated motion in adjacent air-slots is required	Sensor requires removal from deployment to adjust orientation	
	5	4	3	2	1
Application and removal force	<10 lbs.	10–25 lbs.	25–50 lbs.	>50 lbs.	
	5	4	3	2	1
Size	Currently capable of fitting in AZ, SY, AW, AN, AP farm Air-Slot D-D for inspection, or will be mounted on tank sidewall or knuckle	Currently capable of fitting in AY-farm Air-Slot A-A for inspection	Adaptable to AZ, SY, AW, AN, AP farm Air-Slot D-D for inspection with today's materials, electronics, and fabrication practices	Adaptable to AY farm Air-Slot A-A for inspection with today's materials, electronics, and fabrication practices	Not currently adaptable
	5	4	3	2	1
Timeframe for transducer size adaptation	0–3 months	3–6 months	6–9 months	9–12 months	>12 months
	5	4	3	2	1
Cost to adapt	$0–$50K	$50K–$100K	$100K–$200K	$200K–$300K	>$300K
	5	4	3	2	1
Data quality – SNR	>20 dB	10 to 19 dB	5 to 9 dB	<5 dB	
	5	4	3	2	1

Appendix G – Deployment Trade-off Evaluation Criteria and Scoring System

Deployment Trade-off	Criteria and Point Values (not Weighted)				
	5	**4**	**3**	**2**	**1**
Sensitivity to wall thinning	-	Detected WT at reportable and actionable levels	Detected WT at actionable level	Detected WT only above actionable level	Not shown to be sensitive to WT
Ability to detect defects in 90-degree weld confluence ("pinwheel" weld)	-	-	Detected both defects	Demonstrated detection of one defect	Detection of defects in this region not demonstrated
Performance in detection of 'blind' flaws	-	-	Detected both defects	Detected one defect	Detected no defects
Vulnerability to obstructed air-slots	No vulnerability – the inspection technique does not rely on air – slot access	Low vulnerability – the inspection technique requires at least one air-slot to be unblocked 25–50% of the length between the air-slot entrance and the first air-slot transition (up to 9 ft.) in order to inspect up to the first air-slot transition (~17 ft.).	Moderate vulnerability – the inspection technique requires at least one air-slot to be unblocked 75–100% of the length between the air-slot entrance and the first air-slot transition (>13 ft.) in order to inspect a portion of the tank bottom up to the first air-slot transition	High vulnerability –the inspection technique requires two adjacent air-slots that are both unblocked 50–75% of the length between the air-slot entrances and the first air-slot transitions in order to inspect a portion of the tank bottom up to the first air-slot transition	Extreme vulnerability – the inspection technique requires two adjacent air-slots that are both unblocked 75–100% of the length between the air-slot entrances and the first air-slot transitions in order to inspect a portion of the tank bottom up to the first air-slot transition
Potential vulnerability to mill scale	-	-	No foreseen vulnerability based on principles of measurements	At least one measurement will be influenced by mill scale	Multiple measurements will be influenced by mill scale
Potential vulnerability to irregular or pitted coupling surface	-	-	Low risk based on principle of measurements	Medium risk based on principle of measurements	High risk based on principle of measurements
Adaptation risk	Low risk-minor sensor design changes that will not affect key sensor components	Mild risk – minor standard or routine sensor design changes that will affect key sensor components that influence performance	Moderate risk-moderate standard or routine sensor design changes that will affect key sensor components that influence performance	High risk-moderate, experimental changes to key sensor components that influence performance	Very high risk-significant, experimental changes to key sensor components that influence performance

Deployment Trade-off	Criteria and Point Values (not Weighted)				
	5	**4**	**3**	**2**	**1**
Commercial state	COTS components requiring minor adaptation	COTS components requiring moderate adaptation	COTS components requiring significant adaptation	Prototype system with minor modification to sensors	Prototype system with major modification to sensors
Cables/in-tank electronics	No cables required (wireless, battery powered)	No cabling is required under tank	Only a single cable is required under tank	Multiple cables in an umbilical are required under tank	Multiple cables requiring special cable management are required under tank
Replacement cost of in-tank sensors/ components	$1–$5K	$5–$10K	$10–$15K	$15–$20K	over $20K

Appendix H – Raw Scores

Table H.1. Flaw Detection Scores

Machined Surrogate Flaw	Flaw ID	Total Points Available	Air-slot Technology				Remote Technology SwRI
			Penn State		Guidedwave	Innerspec	
			SET	Post-SET			
Pit	P1	3	3		3	3	3
Pit	P2	5	5		5	5	5
Pit	P3	4	4		4	4	4
Notch	N1	4	4		4	4	4
Notch	N2(i)	3	3		3	3	3
Notch	N3(m)	3	3		3	3	---
Wall thinning	T1	3	---	3[(a)]	---	---	---
Pit	P4	2	2		2	2	2
Pit	P5	1	1		1	1	1
Pit	P6	4	4		4	4	4
Pit	P7	3	3		3	3	3
Pit	P8	4	4		4	4	4
Pit	P9	3	3		3	3	---
Pit	P10	4	4		4	4	---
Pit	P11	5	5		5	---	5
Pit	P12	3	3		3	3	3
Notch	N4	4	4		4	4	4
Notch	N5	4	4		4	4	4
Notch	N6	4	4		4	4	4
Notch	N7	5	---	5[(a)]	5	5	---
Wall thinning	T2	2	2		---	2	---
Wall thinning	T3	2	2		2	2	---
Wall thinning	T4	2	2		2	2	---
Pit	B1	2	---		2	2	2
Notch	B2	4	4		4	4	4
Total Points		**83**	**81**		**78**	**75**	**59**
Percent Detected			**98%**		**94%**	**90%**	**71%**

(a) During *Sensor Effectiveness Testing*, Penn State did not report on the 10% wall thinning, T1, and the 50% notch located in the 90-degree weld confluence, N7, due to failure to record the data at the time of testing. After *Sensor Effectiveness Testing*, Penn State acquired additional data on T1 and N7 using the same instrumentation settings used previously and was able to detect both T1 and N7. These data are included in total points.

Table H.2. Sensor Attribute Raw Scores

Sensor Attribute Criteria	Penn State	Guidedwave		Innerspec	SwRI
		SET	Post-SET		
Surface prep requirements	5	5		5	5
Tolerance for loose surface material	5	5		5	5
Sensor weight	5	5		5	2
Couplant requirements	5	3	4[(a)]	5	5
Motion requirements	3	5		5	5
Application and removal force	5	4	3	5	5
Size	5	3		3	5
Time and cost to adapt sensor	7	7		5	4
Data quality -SNR	4	5		4	5
Total Points (Post-SET)	**44**	**42**		**42**	**41**

(a) During "Vulnerability" testing, Guidedwave demonstrated the ability to detect flaws using a dry couplant in lieu of a traditional liquid couplant, which increased their score by one point. The test report is provided in Appendix B of this report.

Table H.3. Deployment Trade-off Raw Scores

Deployment Trade-off	Penn State		Guidedwave		Innerspec		SwRI
	SET	Post-SET	SET	Post-SET	SET	Post-SET	
Wall thinning	4	4[(a,b)]	2		4	3[(b)]	1
Pinwheel region defects	2	3[(a)]	3		3		1
Blind flaws	2		3		3		3
Vulnerability to obstructed air-slots	1		4		3		5
Vulnerability to mill scale	2		3		3		3
Vulnerability to pitted coupling surface	3		1	2[(c)]	3		3
Adaptation risk	5		4		3		2
Commercial state	2		4		3		1
Cables/in-tank electronics	1		3		2		4
Replacement cost of in-tank sensors/ components	4		3		1		3
Total Points (Post-SET)	**27**		**31**		**27**		**26**

(a) During Sensor Effectiveness Testing, Penn State did not report on the 10% wall thinning, T1, and the 50% notch located in the 90-degree weld confluence, N7, due to failure to record the data at the time of testing. After Sensor Effectiveness Testing, Penn State acquired additional data on T1 and N7 using the same instrumentation and settings used previously and was able to detect both T1 and N7. Penn State provided the results in a test report located in Appendix A of this report.

(b) The wall thinning score for both Penn State and Innerspec should have both been a value of 3 during Sensor Effectiveness Testing since they were only able to detect the actionable level thinning (20%). After Sensor Effectiveness Testing, Penn State was able to demonstrated the detection of the 10% wall thinning, T1.

(c) The testing performed by Guidedwave with the dry couplant demonstrated tolerance to rough surfaces, such as pitting, which increased their score by one point. The test report is provided in Appendix B of this report.

Pacific Northwest
NATIONAL LABORATORY

Proudly Operated by **Battelle** *Since 1965*

U.S. DEPARTMENT OF
ENERGY

902 Battelle Boulevard
P.O. Box 999
Richland, WA 99352
1-888-375-PNNL (7665)

www.pnnl.gov